

Transepidermal UV radiation of scalp skin ex vivo induces hair follicle damage that is alleviated by the topical treatment with caffeine

Jennifer Gherardini*,#, Jeannine Wegner*,#, Jérémie Chéret*, Sushmita Ghatak*, Janin Lehmann*, Majid Alam†, Francisco Jimenez†, Wolfgang Funk‡, Markus Böhm§, Natalia V. Botchkareva*, Chris Ward*, Ralf Paus¶***,# and Marta Bertolini*,# 

*#Monasterium Laboratory GmbH, Muenster, Germany, †Mediteknia Skin & Hair Lab, Universidad Fernando Pessoa Canarias, and Medical Pathology Group, IUIBS, Universidad de Las Palmas de Gran Canaria, Las Palmas, Spain, ‡Clinic for Plastic, Aesthetic and Reconstructive Surgery Dr. med. Funk, Munich, Germany, §Department of Dermatology, University of Muenster, Muenster, Germany, ¶Centre for Dermatology Research, University of Manchester, and NIHR Manchester Biomedical Research Centre, Manchester, United Kingdom and **Dr. Phillip Frost Department of Dermatology & Cutaneous Surgery, University of Miami Miller School of Medicine, Miami, FL, USA

Received 4 October 2018, Accepted 7 February 2019

Keywords: caffeine, delivery/vectorization/penetration, ex vivo model, hair growth, hair treatment, UV radiation

Abstract

OBJECTIVES: Although the effect of ultraviolet radiation (UVR) on human skin has been extensively studied, very little is known on how UVR impacts on hair follicle (HF) homeostasis. Here, we investigated how solar spectrum UVR that hits the human skin surface impacts on HF biology, and whether any detrimental effects can be mitigated by a widely used cosmetic and nutraceutical ingredient, caffeine.

METHODS: Human scalp skin with terminal HFs was irradiated transepidermally *ex vivo* using either 10 J/cm² UVA (340–440 nm) + 20 mJ/cm² UVB (290–320 nm) (low dose) or 50 J/cm² UVA + 50 mJ/cm² UVB (high dose) and organ-cultured under serum-free conditions for 1 or 3 days. 0.1% caffeine (5.15 mmol/L) was topically applied for 3 days prior to UV exposure with 40 J/cm² UVA + 40 mJ/cm² UVB and for 3 days after UVR. The effects on various toxicity and vitality read-out parameters were measured in defined skin and HF compartments.

RESULTS: Consistent with previous results, transepidermal UVR exerted skin cytotoxicity and epidermal damage. Treatment with high and/or low UVA+UVB doses also induced oxidative DNA damage and cytotoxicity in human HFs. In addition, it decreased proliferation and promoted apoptosis of HF outer root sheath (ORS) and hair matrix (HM) keratinocytes, stimulated catagen development, differentially regulated the expression of HF growth factors, and induced perifollicular mast cell degranulation. UVR-mediated HF damage was more severe after irradiation with high UVR dose and reached also proximal HF compartments. The topical application of 0.1% caffeine did not induce skin or HF cytotoxicity and stimulated the expression of IGF-1 in the proximal HF ORS. However, it promoted keratinocyte apoptosis in selected HF compartments. Moreover, caffeine provided protection towards UVR-mediated HF

cytotoxicity and dystrophy, keratinocyte apoptosis, and tendential up-regulation of the catagen-promoting growth factor.

CONCLUSION: Our study highlights the clinical relevance of our scalp UV irradiation *ex vivo* assay and provides the first evidence that transepidermal UV radiation negatively affects important human HF functions. This suggests that it is a sensible prophylactic strategy to integrate agents such as caffeine that can act as HF photoprotectants into sun-protective cosmeceutical and nutraceutical formulations.

Résumé

OBJECTIFS: Alors que l'effet de rayons ultraviolets (RUV) sur la peau humaine a été largement étudié, on sait très peu de choses de l'impact des UV sur l'homéostasie du follicule pileux (FP). Ici, nous avons étudié l'effet du spectre des RUV solaires qui atteignent la surface de la peau humaine sur la biologie du FP, et si tout effet nocif peut être atténué par de la caféine, un ingrédient cosmétique et neutraceutique largement utilisé.

MÉTHODES: Une peau de cuir chevelu humain avec ses FP terminaux a été irradiée *ex vivo* via l'épiderme soit par 10 J/cm² d'UVA (340–440 nm) + 20 mJ/cm² d'UVB (290–320 nm) (dose faible) soit par 50 J/cm² d'UVA + 50 mJ/cm² d'UVB (dose élevée) et placée en culture sans sérum pendant 1 ou 3 jours. 0.1% (5.15 mM) de caféïne a été appliquée par voie topique pendant 3 jours avant l'exposition aux UV à raison de 40 J/cm² d'UVA + 40 mJ/cm² UVB et pendant 3 jours après l'exposition aux RUV. Les effets sur divers paramètres de toxicité et de vitalité ont été mesurés au niveau de compartiments définis de la peau et des FP.

RÉSULTATS: Cohérent avec les résultats précédents, les RUV transépidermiques ont exercé une cytotoxicité au niveau de la peau et des lésions épidermiques. Le traitement par des doses élevées et/ou faibles d'UVA+UVB a également induit des lésions oxydatives de l'ADN et une cytotoxicité au niveau des FP humains. En outre, il a diminué la prolifération et favorisé l'apoptose de la gaine externe de la racine (ORS) du FP et des kératinocytes de la matrice des cheveux (MC), a stimulé le développement de la phase catagène, a régulé de manière différentielle l'expression des facteurs de

Correspondence: Dr. Marta Bertolini, Monasterium Laboratory, Skin & Hair Research Solutions GmbH, Nano-Bioanalytik Zentrum, Mendelstraße 17, D-48149 Münster, Germany. Tel: +49 (0) 251 93263-080; fax: +49 (0) 251 93264-457; e-mail: m.bertolini@monasteriumlab.com

#Equally contributed.

croissance des FP, et induit une dégranulation périfolliculaire des mastocytes. Les lésions du FP médiées par les RUV étaient plus graves après une irradiation par dose élevée de RUV et atteignaient également les compartiments proximaux du FP. L'application topique de 0,1 % de caféine n'a pas induit de cytotoxicité de la peau ou du FP et a stimulé l'expression d'IGF-1 dans la partie proximale de l'ORS du FP. Cependant, elle a promu l'apoptose des kératinocytes dans certains compartiments de FP. En outre, la caféine a fourni une protection des FP contre la cytotoxicité et la dystrophie médiées par les RUV, l'apoptose des kératinocytes et une régulation à tendance positive de l'effet catagène induit par le facteur de croissance.

CONCLUSION: Notre étude souligne la pertinence clinique de notre dosage d'irradiation UV *ex vivo* du cuir chevelu et fournit la première preuve que le rayonnement UV transépidermique affecte négativement d'importantes fonctions du FP chez l'homme. Cela suggère que l'intégration d'agents photoprotecteurs des FP tels que la caféine dans les formulations cosmétiques et nutraceutiques des écrans solaires pourrait constituer une stratégie prophylactique sensée.

Introduction

Solar ultraviolet (UV) radiation encompasses three sub-categories of rays of different wavelengths: long wave UVA (320–400 nm), medium wave UVB (280–320 nm), and short wave UVC (100–280 nm). As more than 99% of UVC is absorbed by the ozone layer, only UVA and UVB reach the earth's surface and impact on biological and pathological processes, especially within the organism's integuments (1–3). Although UVA penetrates into the dermis, UVB is almost completely absorbed by the epidermis (2, 4, 5). Though the impact of UVR on the skin stimulates the production of vitamin D, important for tissue homeostasis (6), the combination of UVA and UVB also triggers negative processes which result in erythema, edema, sunburn, photoageing and cancer (1–4, 7–11).

Although the effect of UVA+UVB radiations (UVR) on the epidermis and dermis in mice and human (e.g. (12–17)) has been extensively studied, the effect on skin appendages, such as the hair follicle (HF), has received less attention. This is surprising considering that increased hair loss is reported in patients exposed to repeated episodes of sunburn in the scalp skin (18, 19), and that phototherapy seems to be beneficial for the treatment of selected alopecias (20–23).

Depending on the wavelength and intensity chosen for the experiment, UVR can either promote or inhibit hair growth in rodents (24–27). Transepidermal UVR of mouse skin *in vivo* greatly increased keratinocyte apoptosis in the upper (distal) HF epithelium (28). UVR-mediated HF melanocyte stem cell activation resulted in increased numbers of melanocytes within the epidermis (29). Previously, we showed that microdissected, organ-cultured human scalp HFs exhibit prominent dose-dependent responses to UVB irradiation (20 and 50 mJ/cm²) on the human hair bulb and its surrounding mesenchyme, ranging from apoptosis to necrosis induction, along with down-regulation of hair matrix (HM) keratinocyte proliferation, decrease in intrafollicular adrenocorticotropic hormone production and a striking increase in the number and degranulation of perifollicular mast cells (30). UVB (50 mJ/cm²) exposure also stimulated apoptosis in human dermal papilla fibroblasts, and altered the expression of miRNAs involved in several cell processes, e.g. cell cycle, adhesion, communication and death *in vitro* (31). However, it remains entirely unexplored

how UVR that hits the scalp surface impacts on human HF biology.

To address this major open question in dermatology, we have modified our previously published human full-thickness skin organ culture *ex vivo* assay (32–35) by transepidermally irradiating scalp skin fragments from the skin surface with 10 J/cm² UVA + 20 mJ/cm² UVB (low dose) and 50 J/cm² UVA + 50 mJ/cm² UVB (high dose) within the solar spectrum (340–440 nm UVA and 290–320 nm UVB), and cultured the skin *ex vivo* under serum-free condition for 1 or 3 days. The effect of UVR was evaluated by assessing general tissue cytotoxicity (30, 36), epidermal damage (37), HF cytotoxicity and dystrophy (32, 38), oxidative damage of genomic DNA (30), HF keratinocyte proliferation and apoptosis, anagen catagen transition, the expression of selected growth factors involved in hair cycle control (39–41), and changes in perifollicular mast cell activities (42).

In addition, using this physiological *ex vivo* human skin UV irradiation assay, we assessed whether the topical application (43) of 0.1% caffeine (5.15 mmol/L), a widely used nutraceutical that is also contained as cosmetic ingredient in hair care formulations (44–46), interferes with UVR-induced HF damage. To mimic the experience of consumers using routinely caffeine-based shampoos, skin samples were treated with caffeine for 3 days prior to UV exposure with 40 J/cm² UVA + 40 mJ/cm² UVB and for 3 consecutive days after.

Our interest in this ingredient was based on the fact that caffeine 1) is percutaneously absorbed very easily and also through the HF when topically applied (47–51); 2) ameliorates UVR mediated-skin reactions in murine and human skin (52–56), and 3) regulates several aspects of HF biology, including HF cycling *ex vivo* (57, 58) and *in vivo* (44, 59, 60). In addition, even though caffeine is commonly used in cosmetic hair care formulations and shampoos (44–46), the effect of this nutraceutical after topical application on healthy human scalp HFs *ex vivo* remains to be investigated.

Materials and methods

Human skin samples

For the experiments evaluating the effects of UVR on HF damage, human skin specimens were obtained from either the temporal or occipital scalp regions of two female donors (55 and 66 years old). For the caffeine experiment, skin biopsies were obtained from occipital scalp of two male donors (32 and 56 years old) undergoing hair transplantation. Skin samples were obtained after informed consent and Ethics Committee Approvals (University of Muenster, no. 2015-602-f-S, University of Las Palmas de Gran Canaria, CEIH-2014-06) and treated according to the Helsinki Ethical Guidelines for medical research involving human subjects.

UVA and UVB irradiation experiment

After overnight delivery of the skin sample, 4 mm squared skin biopsies containing terminal HFs were excised using a scalpel under sterile conditions. Skin fragments were placed at air liquid interface within serum-free conditions in a minimal media of William's E media (Thermo Fischer Scientific, Waltham, MA, USA) supplemented with 2 mmol/L of L-glutamine (Thermo Fischer Scientific), 10 ng/mL hydrocortisone (Sigma-Aldrich), 10 µg/mL insulin (Sigma-Aldrich) and 1% penicillin/streptomycin mix (Thermo

(A) Experimental design for UVA and UVB irradiation experiments							
Day -2	Day -1	Day 0		Day 1	Day 2	Day 3	
- Prepare skin fragments - Culture initiation	- Change medium	- Collect medium for LDH assay - Irradiation with respective doses or samples treated as sham - Change medium		- Collect medium for LDH assay - Change medium or embed day 1 samples	- Collect medium for LDH assay - Change medium	- Collect medium for LDH assay - Embed day 3 samples	
(B) Experimental design for Caffeine and UVR experiments							
Day 0	Day 1	Day 2	Day 3	Day 4	Day 5	Day 6	Day 7
- Prepare skin fragments - Culture initiation	- Collect medium for LDH assay - Change medium - Topical application of vehicle or caffeine	- Collect medium for LDH assay - Change medium - Topical application of vehicle or caffeine	- Collect medium for LDH assay - Change medium - Topical application of vehicle or caffeine	- Collect medium for LDH assay - Irradiation with respective doses or samples treated as sham - Change medium - Topical application of vehicle or caffeine	- Change medium - Topical application of vehicle or caffeine	- Collect medium for LDH assay - Change medium - Topical application of vehicle or caffeine	- Collect medium for LDH assay - Change medium - Topical application of vehicle or caffeine

(C)

Viscous vehicle with or without caffeine

Supplemented serum-free William's E Medium

PBS

Plastic ring for protecting sample's edge from UVR

UVA UVB

After 3 days

After UVR

After 3 days

Sample Embedding

Figure 1 Detailed experimental design. (A) Experimental design for UVA and UVB irradiation experiments. (B) Experimental design for caffeine/UVR experiments. (C) Schematic drawing showing the experimental design for caffeine/UVR experiments.

Fischer Scientific) and incubated at 37°C in a humidified atmosphere of 5% CO₂ (32–35,43).

After 2 days of culture (1 day for equilibration, and 1 day for allowing the pre-treatment with UV-protector candidate agents in further experiments), HF containing skin biopsies were transferred to PBS and exposed to solar spectrum UVA and UVB, using an irradiation bank sellasol (System Dr. Sellmeier, 340–440 nm) for UVA and irradiation bank with four TL12 fluorescent lamps (Philips, Eindhoven, The Netherlands, 290–320 nm) for UVB, or treated as sham (no irradiation).

Two different combinations of UVA and UVB doses were used. A high UV dose (50 J/cm² UVA + 50 mJ/cm² UVB), hereby referred to as 'high', and a low dose (10 J/cm² UVA + 20 mJ/cm² UVB), hereby referred to as 'low' of UV was chosen. Since the irradiation bank sellasol (System Dr. Sellmeier) (340–440 nm) has an irradiation capacity of 6.593 J/cm² per min, samples were irradiated for 91 or 455 sec for achieving 10 J/cm² and 50 J/cm² respectively. Given that the irradiation bank with four TL12 fluorescent lamps

(Philips, Eindhoven, The Netherlands) (290–320 nm) has an irradiation capacity of 41.958 mJ/cm² per min, samples were irradiated for 28.6 or 71.5 sec for achieving 20 mJ/cm² and 50 mJ/cm² respectively.

Skin biopsies were cultured in supplemented William's E media for either 1 or 3 days after irradiation and then processed for *in situ* analyses. Culture media was renewed every 24 hours and collected every day for further analysis (Figure 1a).

Caffeine and UVR experiment

4 mm skin biopsies containing terminal HFs were transported in the laboratory on the same day of the surgery. Skin biopsies were placed at air liquid interface within serum-free supplemented William's E media (see above) and incubated at 37°C in a humidified atmosphere of 5% CO₂ (35, 43) (Figure 1b). After 1 day of culture for equilibration, skin biopsies were treated topically with 2 µl of viscous formulation containing PEG6000 prepared in our laboratory, which

enhances test agent penetration and is very viscous thus preventing test compound spill-over from the skin surface into the medium (43) either containing distilled water for the vehicle, and vehicle+UVR group or caffeine 0.1% (5.15 mmol/L) for the caffeine and caffeine+UVR group, for 3 days. At day 4 of organ culture, after 3 days of treatment with caffeine, HF containing skin biopsies were transferred to PBS and only vehicle+UVR and caffeine+UVR groups were exposed to 40 J/cm² UVA + 40 mJ/cm² UVB while vehicle and caffeine groups were treated as sham control without irradiation (Figure 1c). Since the irradiation bank sellasol (System Dr. Sellmeier) (340–440 nm) has an irradiation capacity of 6.593 J/cm² per min, samples were irradiated for 364 sec for achieving 40 J/cm². Given that the irradiation bank with four TL12 fluorescent lamps (Philips, Eindhoven, The Netherlands) (290–320 nm) has an irradiation capacity of 41.958 mJ/cm² per min, samples were irradiated for 57.2 sec for achieving 40 mJ/cm².

Different concentrations of caffeine were previously used to investigate its penetration and effects into porcine *in vitro* (e.g. (61)) or human skin *in vivo* (e.g. (49, 60)) or *in vitro* (e.g. (47)). The concentration of caffeine used for these experiments was carefully selected in order to achieve a local concentration around the HFs within the skin of about 0.001%, a dose that was shown to be beneficial in male HFs (58).

After irradiation, skin samples were placed in supplemented William's E media. Skin biopsies were treated with topical vehicle or caffeine formulation for 3 days prior irradiation, on the day of irradiation and for 3 days after and then further processed for *in situ* analyses. Skin surface was cleaned every day before the topical treatment and culture media was renewed every 24 hours and collected (except for day 5) (Figure 1b). The choice of 40 J/cm² UVA + 40 mJ/cm² UVB dose within the solar spectrum was determined by the fact that in our previous experiments only minor responses were seen with the low UVR regime and that the high UVR regime-treated samples revealed excessive tissue damage that hindered instructive analyses of all HFs within the irradiated skin samples.

LDH (lactate dehydrogenase) assay

Cytotoxicity was studied by lactate dehydrogenase (LDH)-based assay (30, 32, 36, 38) using the Cytotoxicity Detection Kit (Roche Diagnostics GmbH, Mannheim, Germany) following the manufacturer's instructions. Supplemented William's E medium was used as low control, while overnight incubation of skin punch with 0.1% triton X-100 in supplemented William's E medium that causes maximum LDH release was used as high control. LDH measurements were performed using a POLARstar Omega microplate reader (BMG Labtech).

Frozen skin sample processing

Snap frozen samples were sectioned with a cryostat (Leica) and 7 µm sections were collected. The skin sample was carefully orientated to obtain full-length HF sections. Consecutive sections of each full-length HF were collected and slides stored at -80°C (35).

Histochemistry

Haematoxylin and Eosin staining to visualize sunburn cells was performed according to routine histochemical methods and as

described before (28, 62). For the histochemical visualization of melanin, Masson Fontana staining was performed as previously described (38). Toluidine Blue staining was performed to visualize mast cells. Briefly, cryosections were incubated in staining solution (0.1% Toluidine blue) for 1 min. Sections were washed in distilled water, dehydrated and mounted using xylol (42).

Immunohistochemistry

To evaluate proliferating and apoptotic keratinocytes in the epidermis and within the distal (upper), central (mid) and proximal (lower) HF outer root sheath (ORS) as well as in the HM, Ki-67/TUNEL double-staining was performed as previously described (39–41). Briefly, cryosections were fixed with 4% paraformaldehyde in PBS and labelled with a digoxigenin-deoxyUTP (ApopTag® Fluorescein *In Situ* Apoptosis Detection Kit, Merck KGaA, Darmstadt, Germany) in the presence of terminal deoxynucleotidyl transferase, followed by incubation with a mouse anti-Ki-67 antibody (1:800 in PBS; Cell Signalling Technology, Leiden, Netherlands) overnight at 4°C. TUNEL-positive cells were visualized by an antidiigoxygenin fluorescein isothiocyanate (FITC)-conjugated antibody (ApopTag-Fluorescein Detection kit, Merck KGaA, Darmstadt, Germany), whereas the primary antibody against Ki-67 was detected using a rhodamine-labelled goat anti-mouse antibody (1:200, Jackson ImmunoResearch, West Grove, PA).

To evaluate oxidative DNA damage, 8-hydroxy-2'-deoxyguanosine (8-OH-dG) immunostaining was performed as previously published (30). Cryosections were fixed in acetone and blocked with 10% goat normal serum followed by the incubation step with a mouse monoclonal anti-8-OH-dG antibody (1:100 in 2% goat normal serum (GNS) in PBS; Abcam, Cambridge, UK) overnight at 4°C. Secondary antibody incubation with a rhodamine-labelled goat anti-mouse antibody (1:200, Jackson ImmunoResearch, West Grove, PA) was performed at room temperature (RT) for 45 min.

To evaluate IGF-1 protein expression (40,58), tissue cryosections were fixed in acetone and endogenous peroxidases blocked with 3% H₂O₂ in PBS followed by an avidin-biotin blocking step and preincubation with TNB buffer (TrisHCl+NaCl+Casein). Samples were incubated with goat anti-human IGF-1 antibody (1:250 in antibody diluent; Santa Cruz, Texas, USA) overnight at 4°C. Secondary antibody incubation was performed at RT for 45 min before using the Tyramide signal amplification kit (TSA kit, Perkin Elmer).

To evaluate TGF-β2 protein expression (40,58), samples were fixed in methanol and blocked with 10% GNS followed by incubation with a rabbit polyclonal anti-human TGF-β2 antiserum (1:400 in 1% BSA in PBS; Abcam, Cambridge, UK) overnight at 4°C. Secondary antibody incubation using a rhodamine-labelled goat anti-rabbit antibody (1:200, Jackson ImmunoResearch, West Grove, PA) was performed at RT for 45 min.

Negative control for primary antibody was used by omitting terminal deoxynucleotidyl transferase or the primary antibody. Counterstaining to visualize nuclei was performed with 4',6-diamidino-2-phenylindole (DAPI) (Sigma-Aldrich Biochemie GmbH, Hamburg, Germany).

Image capture

Images of the evaluation areas indicated in Figure 2 were taken at original magnifications of 100× or 200× with Keyence-Biozero 8100 and 9100 microscopes (Keyence Corporation, Osaka, Japan) of the evaluation areas indicated below (Figure 2).

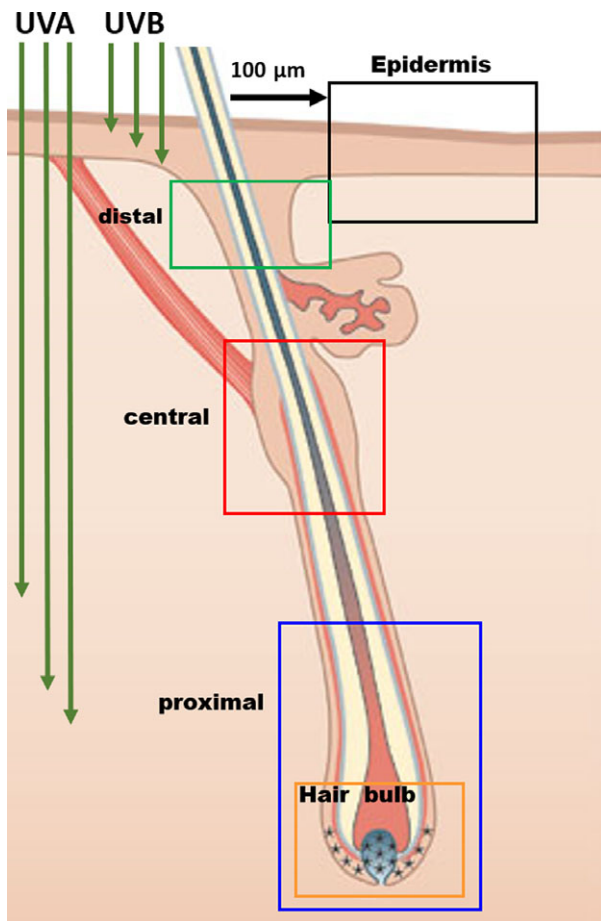


Figure 2 Schematic representation of the different areas evaluated in this study. Epidermis (black box), distal or upper outer root sheath (ORS, green box) also called infundibulum, central ORS (red box) also called bulge/isthmus, proximal or lower ORS (blue box), hair bulb (orange box). (HF picture modified from (63)).

Quantitative (immuno-)histomorphometry

The number of sunburn cells and the % of apoptotic TUNEL⁺ cells among DAPI⁺ cells were quantified within the epidermis of each microscopic field taken at a distance of 100 μm from the hair canal and plotted as number of sunburn cells per microscopic field. Cells with abnormal nuclei shrinkage and "Spiegelei" (poached egg) morphology were defined as sunburn cells keratinocytes (28, 62). To evaluate oxidative stress in the HF, the relative staining intensity of 8-OH-dG within the proximal ORS and HM was measured using ImageJ (30). Melanin pigments were stained as black dots using Masson Fontana; the presence of abnormal large melanin clumping (i.e. melanin positive conglomerates that were larger than keratinocyte nuclei) was counted in the HM up to 10 lines of cells above the end of the dermal papilla (38). Percentage of Ki-67 and TUNEL⁺ cells among total DAPI cells within the upper, central and low ORS and in the HM below (Ki-67) or below and above (TUNEL) the Auber's line was counted (35). The Auber's line is set at the widest dermal papilla diameter (39). IGF-1 and TGF- β

relative staining intensity in the distal, central and proximal ORS was measured using ImageJ (40,58).

For hair cycle staging, HFs were microscopically evaluated using Masson-Fontana histochemistry and Ki-67/TUNEL immunostaining as previously described (35, 64). Hair cycle staging was studied by calculating the % of HFs in each hair cycle phase: anagen VI, early, mid or late catagen. For the hair cycle score, an arbitrary score was attributed to each hair cycle phase: Anagen VI = 100, early catagen = 200, mid catagen = 300, late catagen = 400, and the mean values were plotted in the graph per group (65). Total mast cell number and percentage of degranulated mast cells was evaluated in the perifollicular dermis within a distance of 100 μm around the hair follicle (42).

Statistical analysis

All data are expressed as mean \pm SEM or fold change of mean \pm SEM over sham, and Gaussian distribution of the data was analysed using D'Agostino and Pearson omnibus normality test. Significant differences were analysed using either unpaired Student's *t*-test (comparison between one set of data and sham or vehicle) or One Way ANOVA (comparison between multiple sets of data) for parametric data, or Mann-Whitney test (comparison between one set of data and sham or vehicle) for nonparametric data or Kruskal-Wallis test, and Dunn's test (comparison between multiple sets of data), comparing the results of each tested group using GraphPad Prism 6 (GraphPad Software). $P < 0.05$ was considered statistically significant. To be able to normalize to the respective sham vehicle samples, for number of sunburn cells (Figure 3b), melanin clumping (Figure 4c), proliferative and/or apoptotic cells (Figure 3c, and 5a,b), and mast cells (Figure 7a,b) value counts of "0 cells" were set to 0.0000000001 (=1E-10).

Results

UVR exerts skin cytotoxicity and severe epidermal damage in human skin organ culture

UVR triggers skin cytotoxicity and epidermal damage (1, 30, 37). To confirm the clinical relevance of our improved *ex vivo* model, skin and epidermal UV-mediated responses were analysed. Skin cytotoxicity assessed as LDH release into the medium (30, 32, 36) was highly increased after high-dose but not after low-dose UV-irradiation (Figure 3a). Instead, both UV doses significantly increased the number of sunburn epidermal keratinocytes having pyknotic nuclei (2, 37) (Figure 3b,d), but only high dose UV-irradiation induced acantholysis (Figure 3d). Interestingly, the number of apoptotic keratinocytes was significantly increased only after high dose of UV-irradiation (Figure 3c,e).

These data reveal that the organ culture of human full thickness scalp skin after transepidermal UV irradiation is optimally suited to determine the impact of UVA and UVB in human skin responses.

UVR induces DNA damage in HF epithelium and causes HF dystrophy

UVR is known to induce DNA damage in human skin (4, 66). We have previously shown that 20 mJ/cm^2 UVB irradiation of HFs *ex vivo* promotes oxidative DNA damage in HF epithelium (30). To investigate if topical UVR exposure also induces DNA damage in the HF epithelium, the expression of 8-OH-dG, the oxidized

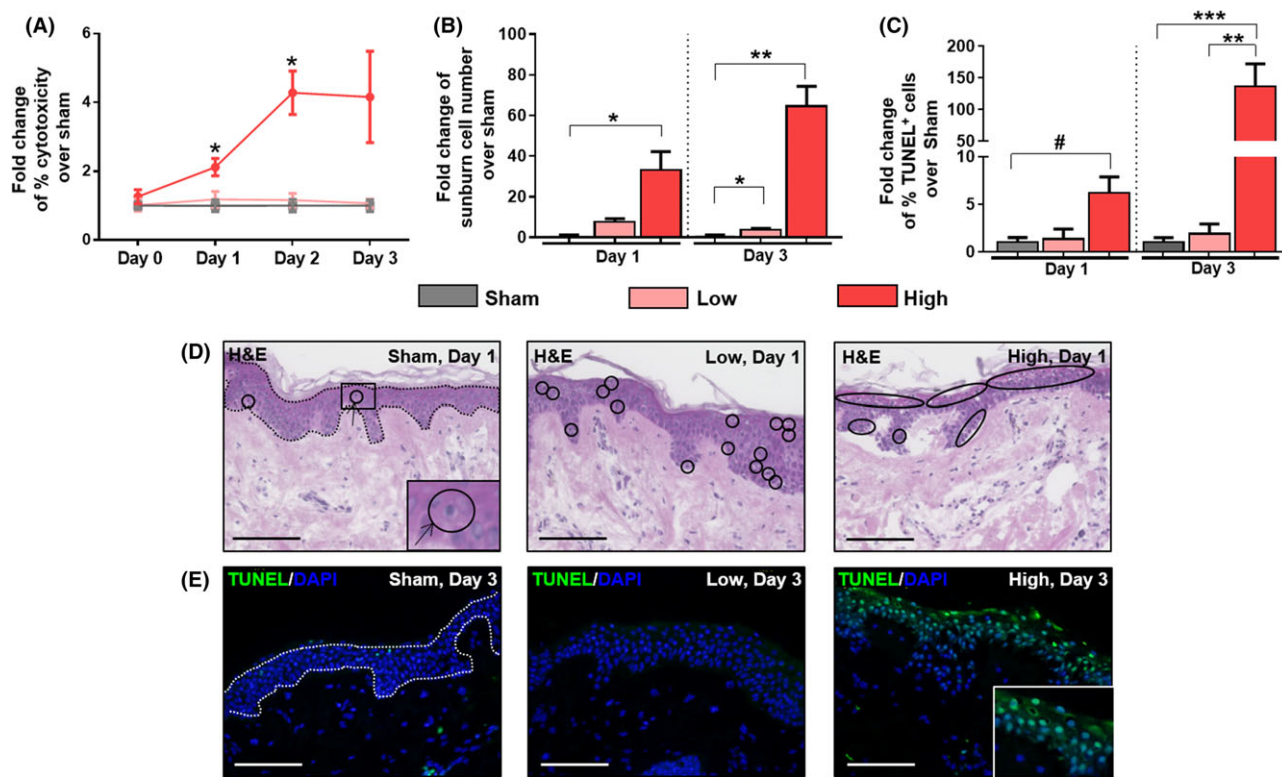


Figure 3 UVR induces skin cytotoxicity and epidermal damage. (A) LDH assay from culture media of skin biopsies treated with sham, high and low dose of UVR. Measurement was performed in triplicates using the supernatant of each biopsy ($n = 2$ skin fragments/group/donor). Data are expressed as fold-change of % cytotoxicity of UVR treated samples over sham. Mean \pm SEM, $n = 4$ medium samples analysed/group from two donors measured in triplicate, Kruskal–Wallis test, $P < 0.05$, and Dunn's test, * $P < 0.05$. (B) Quantitative analysis of the number of sunburn cells in the epidermis of sham, low and high UVR irradiated skin. The number of sunburn cells (circled cells) was counted in the epidermis. Data are expressed as fold-change of sunburn cell number in UVR treated samples over sham. Mean \pm SEM, $n = 12$ –16 evaluation areas analysed from four skin fragments per experimental group from two donors, Kruskal–Wallis test, $P < 0.001$, and Dunn's test * $P < 0.05$, ** $P < 0.01$. (C) Quantitative analysis of the % of TUNEL⁺ keratinocytes in the epidermis of sham, low and high UVR irradiated skin. The number of TUNEL⁺ keratinocytes was counted among all DAPI⁺ cells in the epidermis excluding the stratum corneum and % of TUNEL⁺ cells was calculated. Data are expressed as fold-change of % TUNEL⁺ cell number in UVR treated samples over sham. Mean \pm SEM, $n = 8$ –18 evaluation area analysed from four skin fragments per experimental group from two donors, Kruskal–Wallis test, $P < 0.001$, and Dunn's test ** $P < 0.01$, *** $P < 0.001$, or Mann–Whitney test # $P < 0.05$. (D) Representative images of H&E staining in sham, and low or high irradiated skin. (E) Representative images of TUNEL staining in sham, and low or high irradiated skin. Dotted lines indicate the reference areas used for evaluation (D, E). Scale bars: 100 μ m.

derivative of deoxyguanosine, was investigated (30, 66). Both UVR doses promoted oxidative DNA damage in the HF epithelium, as it was evident from the increase in the nuclear expression of 8-OH-dG in the proximal HF epithelium compartments. However, this effect was more pronounced after treatment with low UVR dose (Figure 4a,b).

Since UV-mediated oxidative stress also contributes to skin cytotoxicity (1), we studied whether UVR penetrating the skin causes HF cytotoxicity and dystrophy by evaluation of melanin clumping in the HF bulb (32, 38). A significant increase in melanin clumping was observed in the hair bulbs on day 3 after low UV irradiation (Figure 4c,d). However, the majority of HFs treated with high UVR lacked of melanin, possibly because of bleaching/oxidative breakdown of the protein (67) or because of premature development of catagen (64), which prevented a meaningful analysis for HF cytotoxicity in this experimental group (Figure 4d).

These data suggest that UVR, most likely UVA penetrating into the dermis, can cause oxidative stress in the HF epithelium, which leads to DNA damage and HF dystrophy.

High dose UVR inhibits keratinocyte proliferation in the infundibulum, promotes apoptosis in the entire HF epithelium, and induces premature catagen development *ex vivo*

It has been demonstrated that UVR induces apoptosis in epidermal keratinocytes (1) and in microdissected HFs that were directly irradiated with UVB *ex vivo* (30). We investigated whether the topical exposure of human skin to UVR would also affect HF keratinocyte proliferation and apoptosis thereby affecting hair growth. Reduction in keratinocyte proliferation was observed only in the upper portion of the ORS (distal) upon irradiation with high UV dose (Figure 5a, c,d). ORS keratinocyte proliferation was also significantly decreased in the central ORS exposed to high UV-irradiated HFs only in one

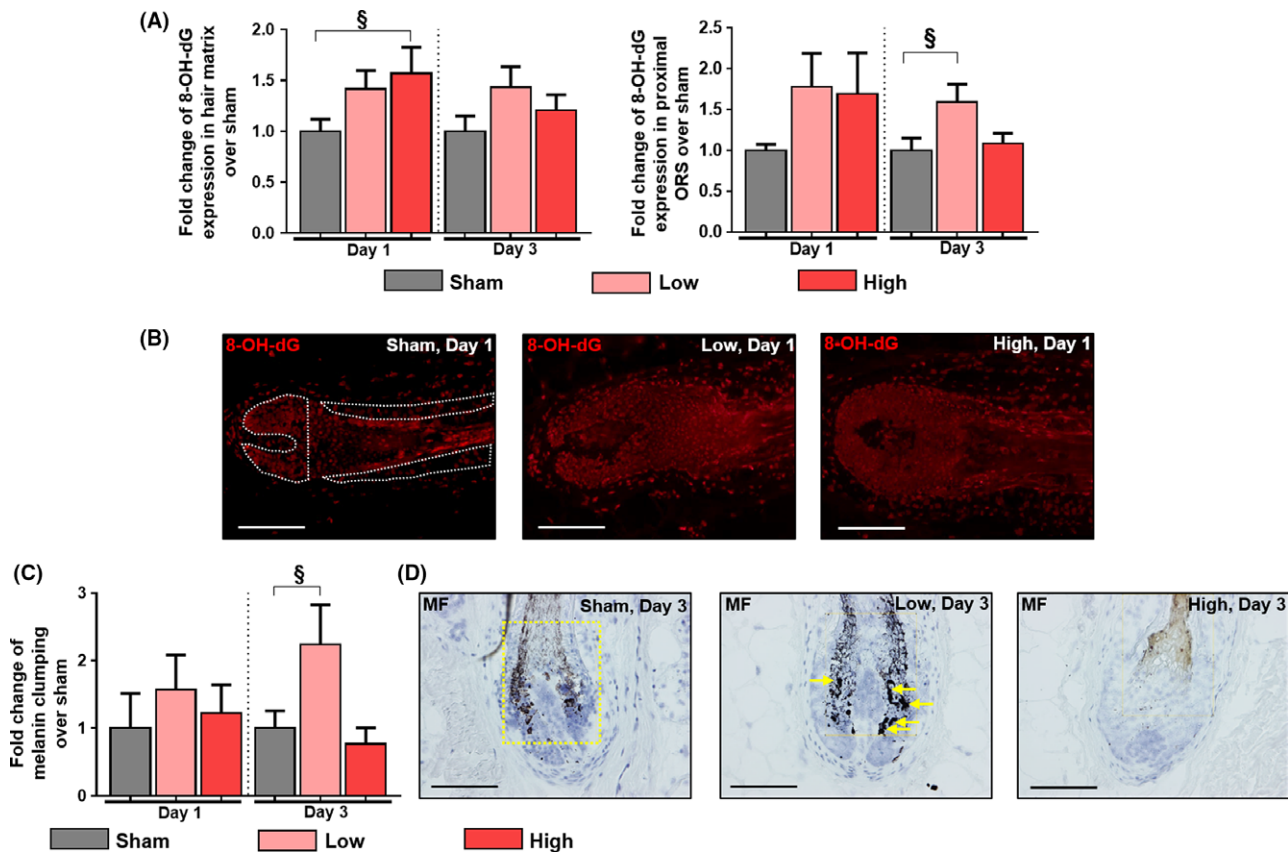


Figure 4 UVR induces DNA damage in the HF epithelium and causes HF dystrophy. (A) Quantitative analysis of 8-OH-dG expression in the proximal ORS and HM of sham, low and high UV irradiated HFs. Relative 8-OH-dG staining intensity was measured using ImageJ. Data are expressed as fold change of 8-OH-dG expression in HM and proximal ORS in UVR treated samples over sham. Mean \pm SEM $n = 8\text{--}15$ for HM and $n = 9\text{--}15$ for proximal ORS areas analysed from four skin fragments per experimental group from two donors. Kruskal-Wallis test, ns, Student's t-test, ${}^{\$}P < 0.05$. (B) Representative images showing 8-OH-dG (red) expression of proximal ORS and HM. (C) Quantitative analysis of melanin clumping using Masson Fontana histochemistry in sham, low and high UV irradiated HFs. Melanin conglomerates that were larger than keratinocyte nuclei were counted in the defined region indicated in yellow. Data are expressed as fold change of melanin clumping of UVR treated samples over sham. Mean \pm SEM $n = 7\text{--}20$ evaluation area analysed from four skin fragments per experimental group from two donors. Kruskal-Wallis test, ns, Student's t-test, ${}^{\$}P < 0.05$. (D) Representative images showing Masson Fontana stained HFs. Arrows indicate melanin clumping. Dotted lines indicate the reference areas used for evaluation (B,D). Scale bars: 100 μm .

donor (data not shown), suggesting that this UV-mediated HF response is possibly subjected to variability between individual donors. However, topical skin exposure to either high or both UVR doses increased the number of apoptotic cells in all analysed HF compartments, including HM, either at day 1 or day 3 or both of organ culture (Figure 5b-d).

The analysis of the hair cycle stages revealed that only high transepidermal UV radiation dose tendentially promoted premature catagen development *ex vivo* (Figure 5e-g). However, the fact that HM keratinocyte apoptosis was significantly increased upon UV low and high irradiation suggests that the observation window used in these experiments may have been too short to observe any significant differences in hair cycle progression.

These data indicate that transepidermal UVR, mainly high UVA, exerts negative effects on HF keratinocytes that reach the most

proximal HF compartment, the hair bulb, thereby possibly stimulating catagen development.

UVR reduces IGF-1 and increases TGF- β 2 protein expression in the outer root sheath keratinocytes

Considering the prominent impact of UVR on HF epithelium, and the fact that high UVR dose stimulates catagen (Figure 5a-g), we were interested in evaluating whether this triggers any changes in the production of growth factors in HF keratinocytes. The protein expression of IGF-1, which is the key anagen prolonging growth factor (40) and of TGF- β 2, the major catagen promoting growth factor (40) were analysed.

Both high and low UVR doses induced a transient up-regulation of IGF-1 expression in the ORS at day 1 after exposure (Figure 6a, c), which may be a compensatory response of the HF against UV-

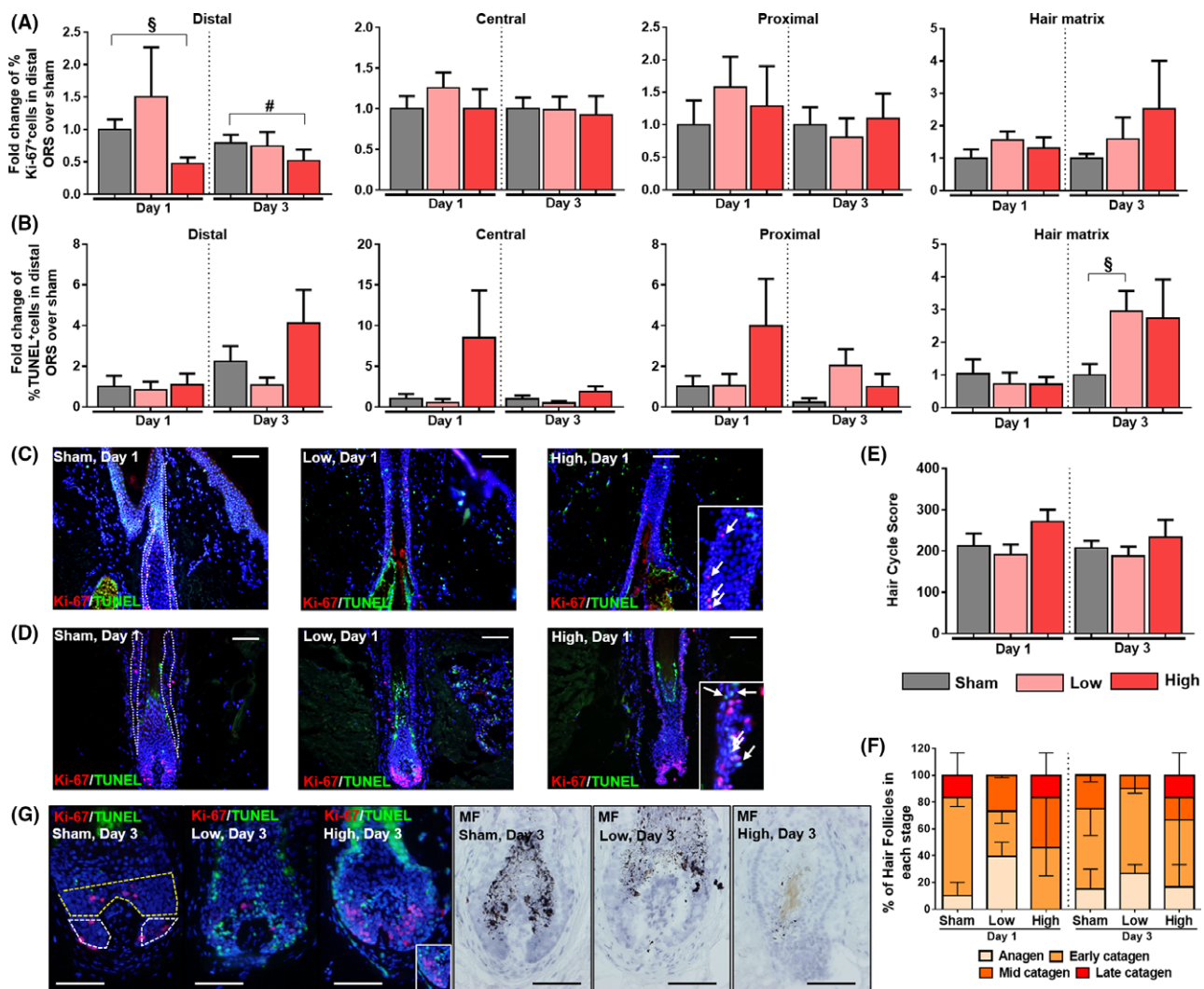


Figure 5 High UVR decreases keratinocyte proliferation in the infundibulum but significantly increases keratinocyte apoptosis, and slightly induces premature catagen development. (A,B) Quantitative analysis of the fold change of the % of Ki-67⁺ (A) and TUNEL⁺ (B) keratinocytes in distal, central, proximal ORS, and HM of sham, low and high UV irradiated HFs. The number and % of Ki-67⁺ or TUNEL⁺ keratinocytes was counted among all DAPI⁺ cells. Data are expressed as fold-change of % Ki-67⁺ or TUNEL⁺ cell number in UVR treated samples over sham. Mean \pm SEM $n = 9-16$ for distal ORS, $n = 16-26$ for central ORS, $n = 8-17$ for proximal ORS, and $n = 7-14$ for HM evaluation area analysed from four skin fragments per experimental group from two donors. Ki-67 distal: Kruskal-Wallis test, $P < 0.05$, and Dunn's test ns, Mann-Whitney test $^{\$}P < 0.05$, or Student's t-test $^{#}P < 0.05$, TUNEL proximal: Kruskal-Wallis test $P < 0.01$, Dunn's test, ns, TUNEL HM: Kruskal-Wallis test, ns, Student's t-test $^{\$}P < 0.05$. (C-D) Representative images showing Ki-67 (red) and TUNEL (green) positive cells in the distal (C) and proximal HF ORS (D), and in the HM. Original magnification: 100 \times or 200 \times . Arrows in inset indicate proliferating Ki-67⁺ cells in distal ORS, and TUNEL⁺ cells in proximal ORS. (E-G) Hair cycle analysis was performed using Ki-67/TUNEL immunohistochemistry and Masson Fontana histochemistry (G). For the hair cycle score, arbitrary units were used to define anagen (100), early catagen (200), mid catagen (300) and late catagen (400). For hair follicle staging, % of HFs in each stage are presented. Data are expressed as Mean \pm SEM $n = 6-15$ HFs for hair cycle score and $n = 2$ donors from 6 to 15 HFs for HF stage analysed from four skin samples per experimental group from two donors. Kruskal-Wallis test, ns. Dotted lines indicate the reference areas used for evaluation (C,D,G). Hair matrix keratinocyte proliferation was evaluated only within the area limited by white dotted line, while hair matrix keratinocyte apoptosis was evaluated within the areas limited by white and yellow dotted lines (G). Scale bars: 100 μ m.

induced oxidative stress (68–70). Long-term effect (day 3 of organ culture) of UVR resulted in decreased expression of IGF-1 expression in the HF epithelium but only upon irradiation with the high dose (Figure 6a,c). In contrast, TGF- β 2 expression was increased

in the HF already at day 1 after UV irradiation and remained high (Figure 6b,d). Therefore, the UVR exposure of skin influences the production of hair cycle-regulating growth factors in the HF epithelium.

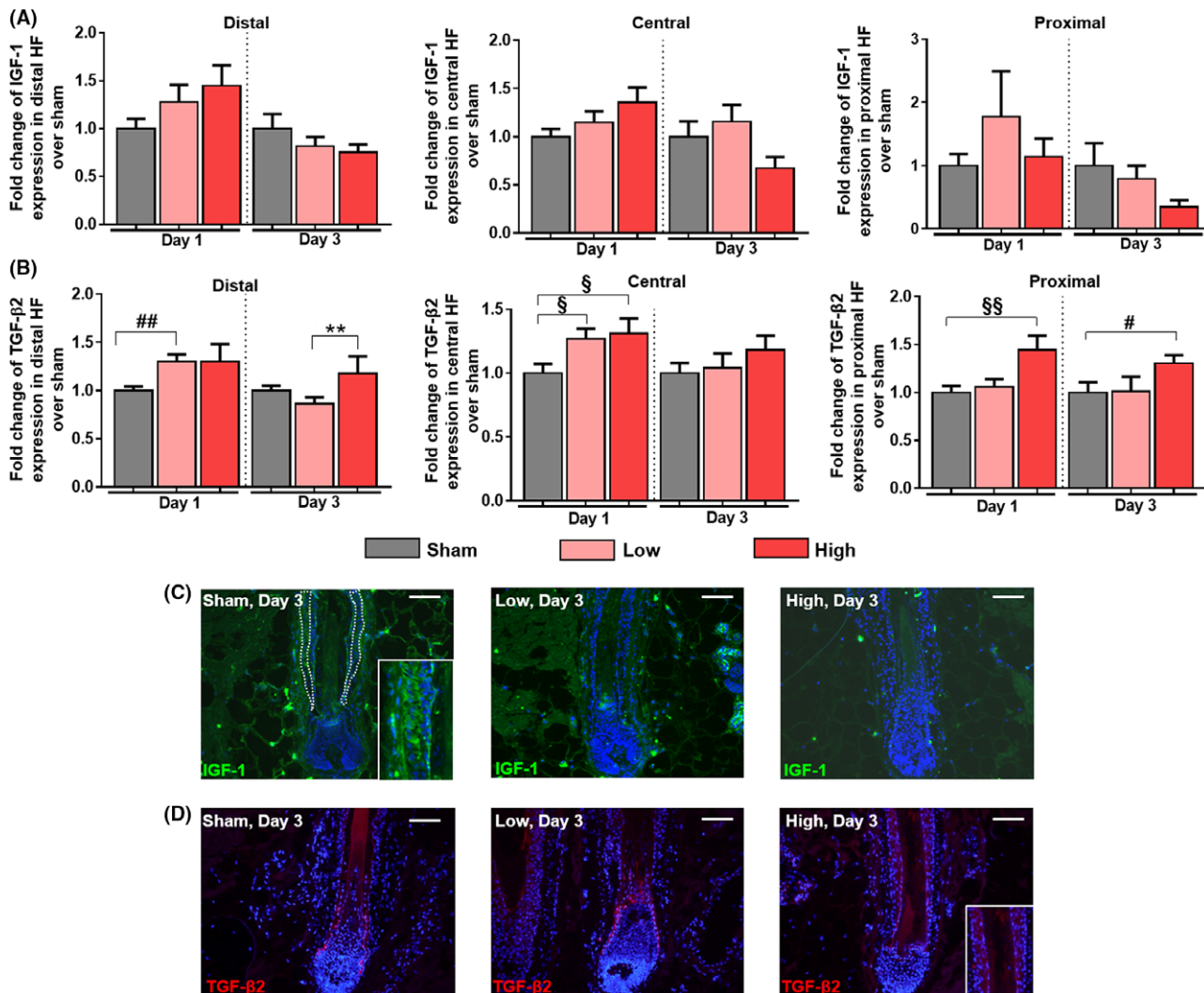


Figure 6 UVR negatively impacts on the expression of hair-cycle regulating growth factors in human scalp HFs. (A) Quantitative analysis of IGF-1 expression in distal, central and proximal ORS of sham, low, and high UV irradiated HFs. Relative IGF-1 staining intensity was measured using ImageJ. Data are expressed as fold-change of IGF-1 expression in UVR treated samples over sham. Mean \pm SEM $n = 5\text{--}15$ for distal ORS, $n = 4\text{--}18$ for central ORS, and $n = 2\text{--}9$ for proximal ORS evaluation area analysed from four skin fragments per experimental group from two donors. IGF-1 distal: Kruskal–Wallis test $P < 0.05$, Dunn's test, ns. (B) Quantitative analysis of TGF- β 2 expression in distal, central and proximal ORS of sham, low, and high UV irradiated HFs. Relative TGF- β 2 staining intensity was measured using ImageJ. Data are expressed as fold-change of TGF- β 2 expression in UVR treated samples over sham. Mean \pm SEM $n = 8\text{--}23$ for distal ORS, $n = 9\text{--}18$ for central ORS, and $n = 10\text{--}18$ for proximal ORS area analysed from four skin fragments per experimental group from two donors. TGF- β 2 distal: Kruskal–Wallis test $P < 0.05$ and Dunn's test, ** $P < 0.01$, Mann–Whitney test $^{**}P < 0.01$, TGF- β 2 center: Kruskal–Wallis test $P < 0.05$ and Dunn's test, ns, Student's *t*-test $^{\$}P < 0.05$, TGF- β 2 proximal: Kruskal–Wallis test $P < 0.05$ and Dunn's test, ns, Mann–Whitney test $^{\#}P < 0.05$ and Student's *t*-test $^{\$\$}P < 0.01$. (C) Representative images showing IGF-1 (green) expression in the proximal hair follicle ORS. (D) Representative images showing TGF- β 2 (red) expression in the proximal hair follicle ORS. Dotted line indicate the reference areas used the evaluation (C). Scale bars: 100 μ m.

Acute HF responses to UVR include the degranulation of perifollicular mast cells

Mast cells are important regulators of hair growth (71–73) and may be functionally important for the maintenance of human HF immune privilege (42) and HF responses to oxidative damage (74). It has been shown that mast cells are highly affected by UVR (75, 76), and that UVR or psoralen plus UVA therapy can be beneficial

for patients affected by mast cell-driven skin disorders (76, 77). Therefore, we were particularly interested in how low or high UVR modulates perifollicular mast cell activities, i.e. number and degranulation of fully matured mast cells.

Toluidine blue staining was used to visualise and quantify the number of mast cells in skin samples exposed to UVR (Figure 7a–d). A significant decrease in the number of histochemically stainable (i.e., mature) perifollicular mast cells (at low UVR dose, except

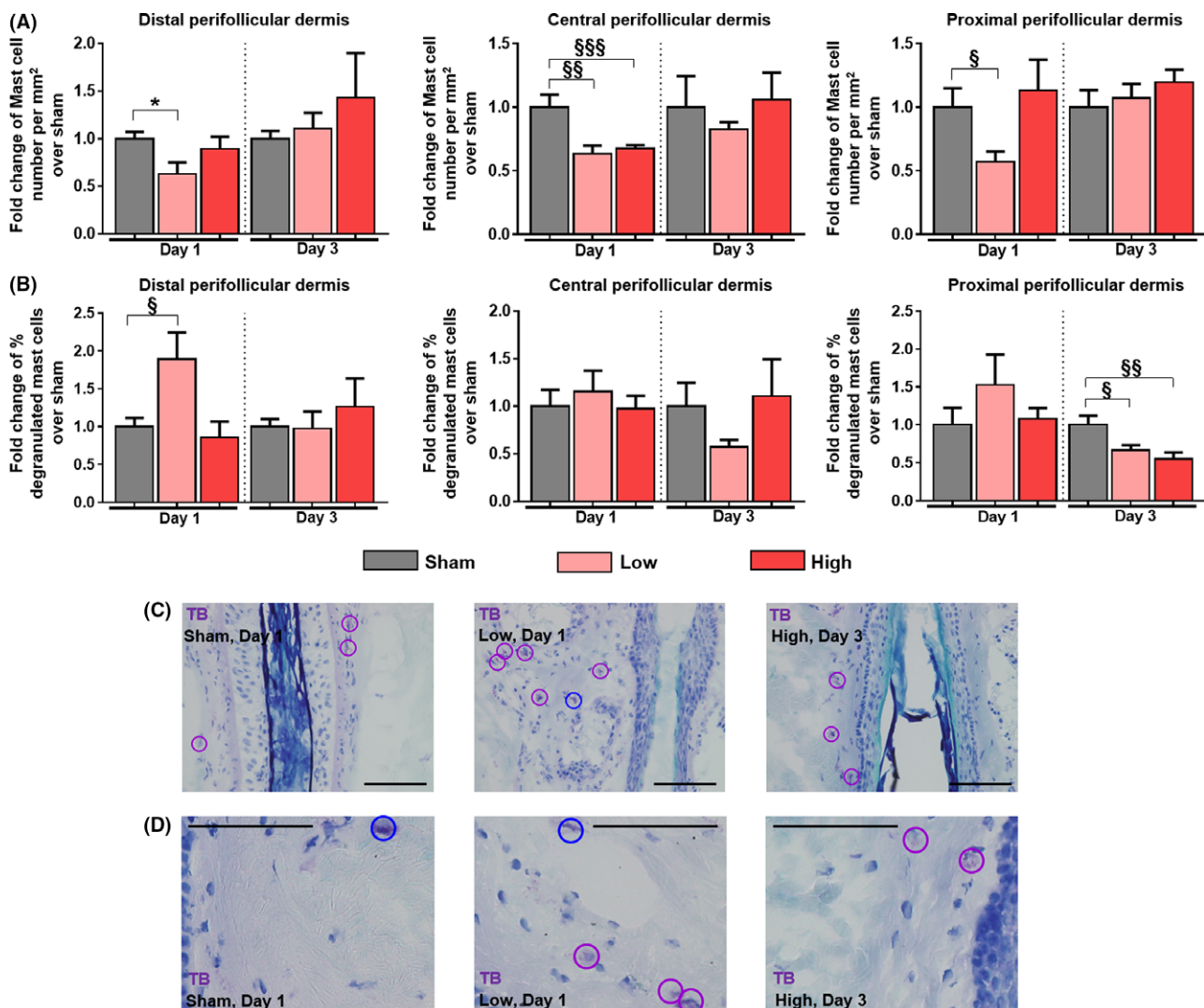


Figure 7 UVR regulates perifollicular mast cell activities. (A) Quantitative analysis of mast cell number in the perifollicular dermis of sham, low and high UV irradiated HFs. Mast cells were counted in an evaluation area of 100 μm from the hair follicle basement membrane and the total number of mast cells per mm^2 was calculated. Data are expressed as fold-change of mast cell number in UVR-treated samples over sham. Mean \pm SEM $n = 7$ –17 for distal, $n = 7$ –18 for central and $n = 11$ –18 for proximal evaluation areas analysed from four skin fragments per experimental group from two donors, distal: Kruskal–Wallis test $P < 0.05$ and Dunn's test, * $P < 0.05$, central: Kruskal–Wallis test ns, Student's t -test, §§ $P < 0.01$, §§§ $P < 0.001$, proximal: Kruskal–Wallis test $P < 0.05$ and Dunn's test, ns, Student's t -test, § $P < 0.05$. (B) Quantitative analysis of % of degranulated mast cells in the perifollicular dermis of sham, low and high UV irradiated HFs. Mast cells were counted in an evaluation area of 100 μm from the hair follicle basement membrane and % of degranulated mast cells out of total was calculated. Data are expressed as fold-change of % of degranulated mast cells in UVR-treated samples over sham. Mean \pm SEM $n = 7$ –17 for distal, $n = 7$ –18 for central and $n = 11$ –18 for proximal area analysed from four skin fragments per experimental group from two donors, distal: Kruskal–Wallis test $P < 0.05$ and Dunn's test, ns, proximal: Kruskal–Wallis test $P < 0.05$ and Dunn's test, ns, Student's t test, § $P < 0.05$, §§ $P < 0.01$. (C–D) Representative images showing toluidine blue histochemistry, non-degranulated (blue circle), degranulated (violet circle). Scale bars: 100 μm .

in the central perifollicular dermis) and increase in mast cell degranulation (at low UVR dose) were detected 1 day after UVR treatment. This effect was diminished 2 days later (Figure 7a,b). However, we noted a major inter-donor variability as UV-induced mast cell degranulation was more prominent in the first donor as compared to the second donor analysed (data not shown).

Taken together, our data show that the combination of UVA and UVB impacts on the HF physiology, and perifollicular mast cell activities.

Topical application of caffeine significantly reduces UV-induced skin cytotoxicity and epidermal keratinocyte damage

To confirm the clinical relevance of our scalp UV irradiation *ex vivo* assay, we investigated whether caffeine protects from skin cytotoxicity and epidermal keratinocyte from UVR-mediated damage, as reported in literature using other experimental approaches (52–56). For the following experiments investigating the protective role

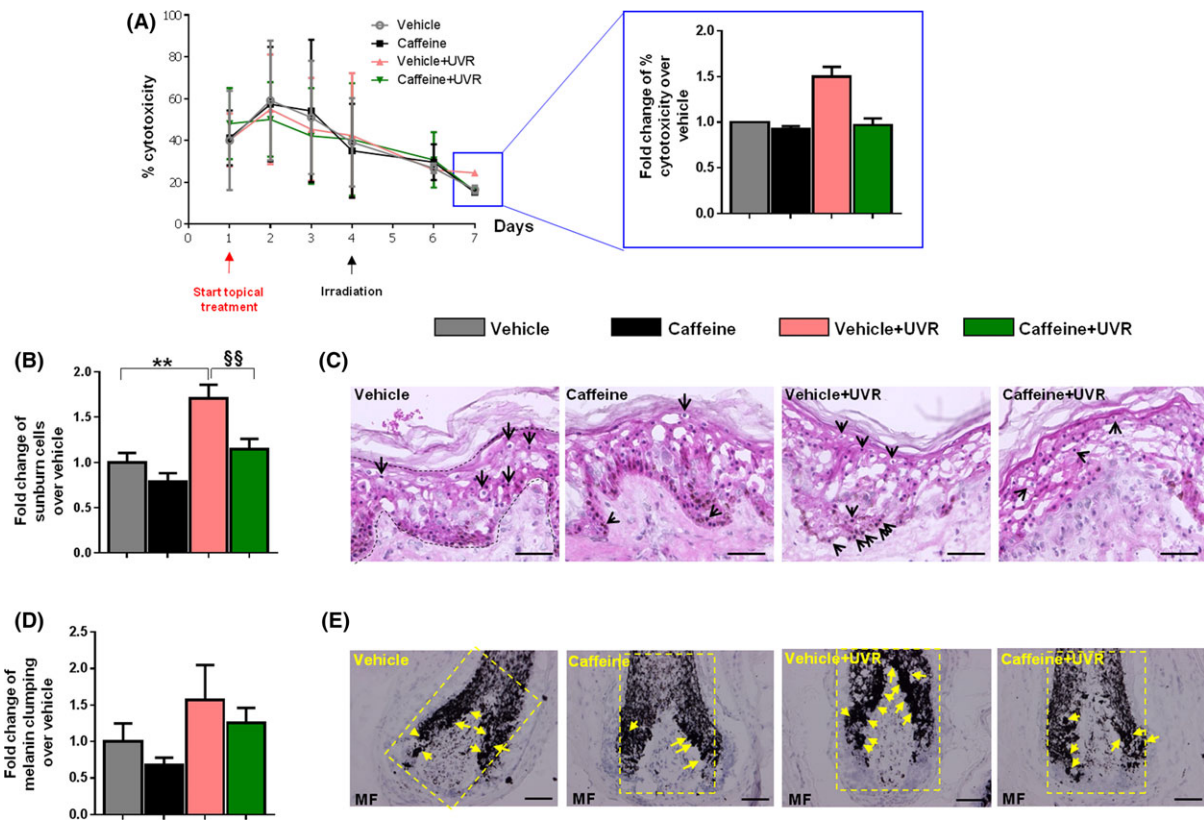


Figure 8 Protective effect of caffeine against UVR-induced skin cytotoxicity, epidermal damage and hair follicle dystrophy. (A) LDH assay from culture media of skin biopsies treated with vehicle, caffeine, vehicle+UVR or caffeine+UVR. Measurement was performed in triplicates using the supernatant of each biopsy ($n = 1$ biopsies/group/donor). Mean \pm SEM or fold-change of Mean \pm SEM over vehicle, $n = 2$ medium samples analysed/group from two donors measured in triplicates. Kruskall–Wallis test, ns. (B) Quantitative analysis of the number of sunburn cells (cells indicated with arrows) in the epidermis of vehicle, caffeine, vehicle+UVR, or caffeine+UVR treated skin. The number of sunburn cells was counted in the epidermis. Data are expressed as fold-change of Mean \pm SEM over vehicle, $n = 11\text{--}20$ evaluation areas analysed from two skin punches per experimental group from two donors, Kruskal–Wallis test $P < 0.05$ and Dunn's test, ** $P < 0.01$, Student's *t* test, §§ $P < 0.01$. (C) Representative images of H&E staining in vehicle, caffeine, vehicle+UVR and caffeine+UVR treated skin. (D) Quantitative analysis of melanin clumping using Masson Fontana histochemistry in vehicle, caffeine, vehicle+UVR or caffeine+UVR treated HFs. Melanin conglomerates that were larger than keratinocyte nuclei were counted in the defined region indicated in yellow. Data are expressed as fold-change of Mean \pm SEM over vehicle, $n = 7\text{--}11$ evaluation areas analysed from two skin punches per experimental group from two donors. One Way-ANOVA, ns. (E) Representative images showing Masson Fontana stained HFs. Arrows indicate melanin clumping in merged images. Dotted lines indicate the reference areas for evaluation (C,E). Scale bars: 50 μm .

of caffeine against UVR-mediated detrimental effects, scalp skin samples rich in terminal HFs from two healthy donors were treated topically with caffeine once a day for six consecutive days *ex vivo* and irradiated on day 3 of organ culture (Figure 1b,c). This set up was selected for mimicking consumer behaviour with caffeine-based shampoo before and after sunbathing. An intermediate dose of UVA+UVB, i.e. 40 J/cm² UVA + 40 mJ/cm² UVB was used in this experiment (for details, see materials and methods).

In line with our previous findings (32), the prolonged culture period selected for this specific assay, which had to be chosen to allow the pre-, and post-treatment with caffeine, was associated with slowly progressing tissue degeneration independent of UVR treatment as shown by histology (Figure 8c). Despite this, our data showed that caffeine protects/reverses skin samples from UVR-induced cytotoxicity, as indicated by the measurement of LDH release into the medium (Figure 8a). In addition, caffeine

protected/rescued epidermal keratinocytes from UVR-induced damage, as the number of sunburn cells was significantly reduced in the epidermis of caffeine pre-treated skin (Figure 8b,c). As expected, but confirmed here for the first time *ex vivo*, the topical application of caffeine does not induce skin or epidermal cytotoxicity (Figure 8a–c).

These data reinforce the clinical relevance of our model and provides the first evidence that this assay can be used to investigate and experimentally manipulate UVR responses in human skin.

Topical application of caffeine does not induce HF cytotoxicity/dystrophy and may tendentially reduce it when this is UVR-mediated

Previously, it was shown that only selected concentrations of caffeine beneficially regulate HF functions (58). Therefore, we wanted

to investigate the safety of caffeine concentration used topically for this study (0.1%, 5.15 mmol/L) and whether it protects HFs from UVR-mediated cytotoxicity/dystrophy.

The topical application of caffeine onto cultured skin *ex vivo* did not induce HF cytotoxicity but rather slightly reduced culture-mediated stress in the HF, as the number of melanin clumps in caffeine treated samples was lower as compared to the vehicle control (Figure 8d,e). In addition, the evaluation of melanin clumps in the HM suggested that caffeine tendentially protected against HF cytotoxicity induced by UVR (Figure 8d,e). These data indicate that caffeine protects from/reverses UV-induced damage not only in the epidermis, as already reported (52–54, 56, 78), but also in the HF epithelium.

Topical treatment with caffeine significantly reduces UVR-induced HF keratinocyte apoptosis *ex vivo*

We have shown that high dose of UVR decreases proliferation and promotes apoptosis of ORS keratinocytes (Figure 5a-d). Therefore, we next investigated whether the continuous topical treatment with caffeine before and after irradiation rescues from UVR-induced deleterious response in the HF epithelium. Importantly, in contrary to the high UVR dose (50 J/cm² UVA and 50 mJ/cm² UVB) and the experimental design employed for the first part of the study (Figure 5a-d), the combination of 40 J/cm² UVA and 40 mJ/cm² UVB slightly induced keratinocyte proliferation in the infundibulum or central HF ORS (Figure 9a,c,d).

However, the combination of 40 J/cm² UVA and 40 mJ/cm² UVB also induced massive keratinocyte apoptosis throughout the ORS, as compared to vehicle sham-treated samples (Figure 9b-d). Significantly reduced percentage of TUNEL⁺ cells in the distal and central parts of the ORS were observed in the HFs that were co-treated with caffeine and UVR, in contrast to the irradiated HFs without caffeine (vehicle+UVR) (Figure 9b-d). The topical treatment with 0.1% caffeine increased the proliferation of HF ORS keratinocytes in the infundibulum (distal) (Figure 9a,c,d) but, quite unexpectedly, also promoted HF keratinocyte apoptosis under the conditions of this *ex vivo* assay, especially in the central and proximal epithelium (Figure 9b-d). Interestingly, in the central ORS, keratinocyte proliferation was lower in caffeine+UVR treated HFs as compared to single administration of caffeine, vehicle+UVR, or vehicle (Figure 9a,c,d).

These data show that the local concentration of caffeine originated by topical administration differentially regulates ORS keratinocyte proliferation and apoptosis. Most importantly, in the current context, they demonstrate that caffeine successfully decreases UV-mediated increased keratinocyte apoptosis in the distal and central ORS.

Caffeine or UVR each differentially impacts on hair cycle-associated parameters but their combination restores baseline levels, thereby leaving hair cycle unaffected *ex vivo*

We have shown above that UVR exposure to the skin surface, namely the combination of 50 J/cm² UVA and 50 mJ/cm² UVB, regulated HM keratinocyte proliferation and apoptosis, slightly induced premature catagen development (Figure 5e-h), and regulated intrafollicular expression of IGF-1, and TGF- β 2 (Figure 6a-d) *ex vivo*. Since caffeine has been shown to prevent catagen development in microdissected HFs *ex vivo* (57, 58) but also *in vivo* (44, 59), we were particularly intrigued to investigate whether the

topical application of 0.1% caffeine prevents/restores UVR-mediated effects in the HM, and proximal ORS.

Caffeine treatment alone significantly up-regulated IGF-1 expression, although skin exposure to the combination of 40 J/cm² UVA and 40 mJ/cm² UVB showed a trend towards increase expression of both IGF-1 and TGF- β 2 expression in the proximal HF ORS (Figure 10a-c). The minimal UV-mediated increase of TGF- β 2 immunoreactivity in the proximal ORS was reversed by caffeine treatment (Figure 10a,c).

Analysis of proliferation and apoptosis in the HM revealed that the combination of 40 J/cm² UVA and 40 mJ/cm² UVB did not have a significant effect, while topical treatment with 0.1% caffeine significantly increased the number of apoptotic cells in the HM (Figure 10d,e). However, most importantly, in HFs treated with caffeine before and after UV irradiation, the apoptosis of HM keratinocytes was restored to baseline level (Figure 10d,e). This, in turn, prevented any significant changes in the number of HFs in anagen or catagen among all treated samples (Figure 10e-g). This suggests that topical caffeine may ensure that hair cycle is not negatively affected by UVR.

Discussion

Our results confirmed previously published data that UVA and UVB induce skin cytotoxicity and epidermal keratinocyte damage. In addition, we demonstrated that transepidermal UVA and UVB irradiation promotes HF cytotoxicity, dystrophy, oxidative DNA damage, decreases keratinocyte proliferation and increases their apoptosis, stimulates the production of TGF- β 2 and the decrease of IGF-1 expression in ORS keratinocytes, triggers premature catagen development, and induces perifollicular mast cell degranulation. UVR-mediated HF damage is more severe after irradiation with high UVR dose and is not only seen in HF compartments close to the skin surface but also in lower regions of HFs, including the hair bulb. The topical application of 0.1% caffeine independently exerts negative effects on the HFs, i.e. keratinocyte apoptosis in selected compartments, but does not induce skin or HF cytotoxicity, and stimulates positive responses in the ORS of treated HFs, such as increased IGF-1 expression. In addition, the topical application of 0.1% caffeine provides protection towards UV-induced HF damage, e.g. UV-mediated HF cytotoxicity and dystrophy, keratinocyte apoptosis in the distal and central ORS, and increased expression of TGF- β 2.

Therefore, our study provides the first evidence that transepidermal UVR negatively modulates important human HF functions, including hair growth. In addition, it advocates a sensible prophylactic strategy to integrate agents into sun-protective cosmeceutical and nutraceutical formulations, such as caffeine, that can act as HF photoprotectants.

Our study also highlights the clinical relevance of the scalp UV irradiation *ex vivo* assay developed in our lab, to simulate, interrogate and experimentally manipulate the complex responses of human skin and its appendages, i.e. HFs, to sunlight and promises important new insights on how topically administered cosmeceuticals impacts on these. In line with previous results *in vivo* (1, 4), UV radiation induces skin cytotoxicity, and epidermal damage in our model. In addition, in our model, in concurrence to previous reports (52–54, 56, 78), caffeine protects/reverses most of such effects. Caffeine penetrates very easily into the skin and thus is routinely used as positive control for penetration studies. In addition, the fact that the topical application of 0.1% caffeine modulates HF-

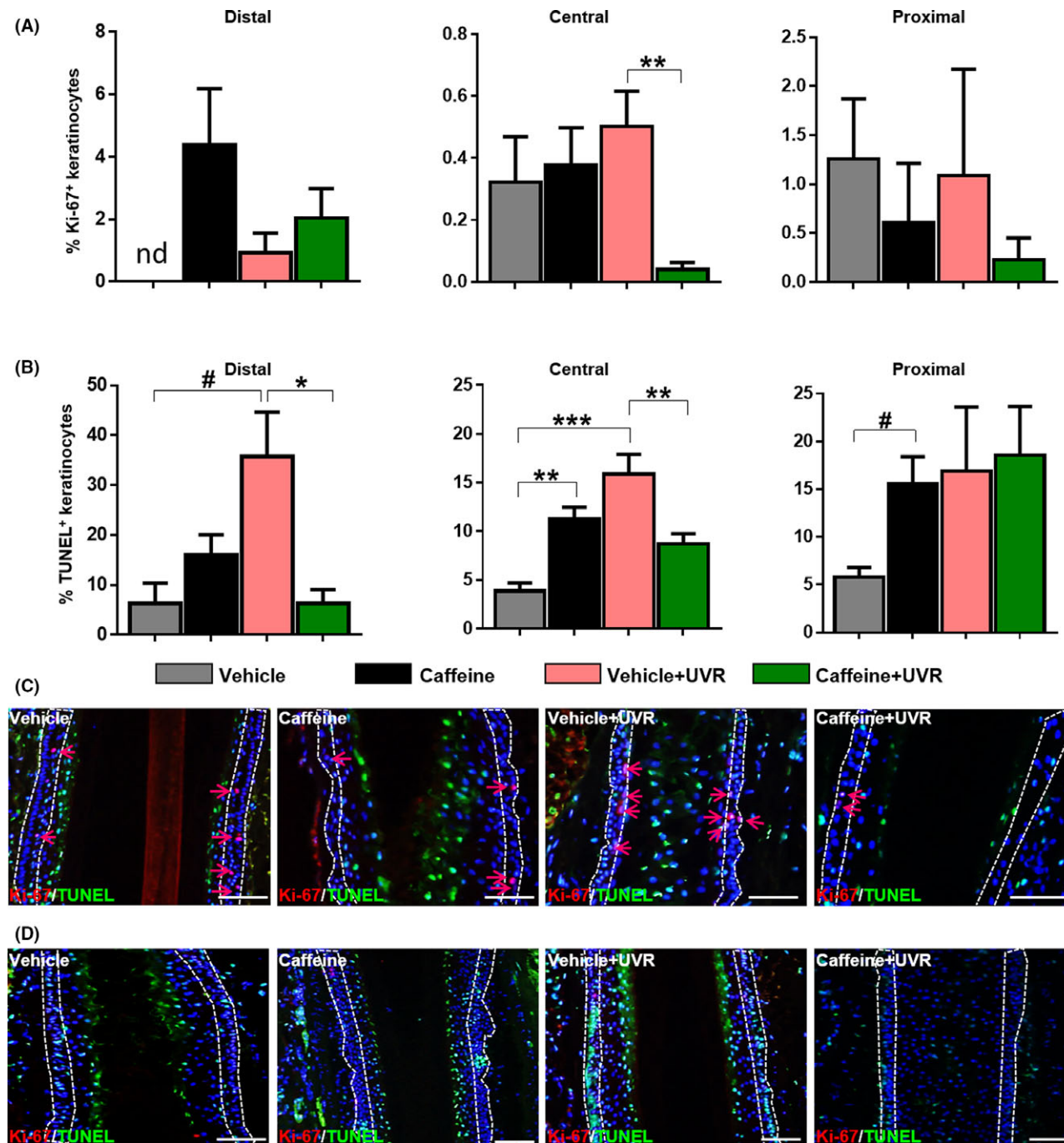


Figure 9 Caffeine protects from UV-induced keratinocyte apoptosis in the HF ORS but also may stimulate it if applied alone. (A–B) Quantitative analysis of the % of Ki-67⁺ (A) and TUNEL⁺ (B) keratinocytes in distal, central, and proximal ORS of vehicle, caffeine, vehicle+UVR or caffeine+UVR treated HFs. The number of Ki-67⁺ or TUNEL⁺ keratinocytes was counted among all DAPI⁺ cells and % of Ki-67⁺ or TUNEL⁺ cells was calculated. Data are expressed as Mean \pm SEM n = 5–10 for distal ORS, n = 11–26 for central ORS, and n = 4–11 for proximal ORS evaluation area analysed from two skin punches per experimental group from two donors, Ki-67 distal: Kruskal–Wallis test, ns, Ki-67 central: Kruskal–Wallis test, P < 0.05 and Dunn's test, **P < 0.01, Ki-67 proximal: Kruskal–Wallis test, ns; TUNEL distal: Kruskal–Wallis test, P < 0.05 and Dunn's test, *P < 0.05, Mann–Whitney test, #P < 0.05, TUNEL central: Kruskal–Wallis test, P < 0.05 and Dunn's test, **P < 0.01, ***P < 0.001, TUNEL proximal: Kruskal–Wallis test, ns, Mann–Whitney test, #P < 0.05. (C–D) Representative images showing Ki-67 (red) and TUNEL (green) positive cells in the distal (C) and proximal (D) hair follicle ORS. Arrows indicate proliferating Ki-67⁺ cells in distal ORS. Dotted lines indicate the reference areas used for evaluation (C,D). Scale bars: 50 μ m. nd, not detected.

related parameters also in the lower epithelium, including in the hair bulb, reinforces the appropriateness of our vehicle formulation for topical application studies.

Daily doses of UV radiation are highly variable because of latitudinal changes (79, 80). The doses of UV radiation chosen for these experiments are comparable to sunlight exposures in Europe in July (81, 82). Namely, 10 J/cm² (low) and 50 J/cm² (high) UVA doses correspond, respectively, to 22–40 min and 109–200 min of midday summer sunlight in France in July. 20 mJ/cm² (low) and 50 mJ/cm² (high) UVB doses correspond, respectively, to 22–30 min and 56–73.5 min of sunlight in July in Germany. Considering that hair themselves absorb UV radiation (83–85), the impact of UVA and UVB on the scalp skin is usually reduced. However, this is not the case in patients suffering from skin barrier defects (86), lipid production deregulation (87), or alopecia, where the scalp skin surface is totally exposed to sunlight and to sunburn (88).

Though we have detected UV-mediated damage throughout the HF length, this is more prominent in the upper layers of the skin (distal HF), as compared to the lower HF (central and proximal). The reason must depend on the fact that although the upper part of the HF is hit by both UVA and UVB, only UVA penetrates very deeply into the skin and can be absorbed by the hair bulb. Therefore, the negative impact of UV radiation on the lower HF, including induction of catagen, is triggered either by an indirect effect of UVB on infundibulum keratinocytes, which in turn exerts knock-on effects to lower HF compartments, or most likely by a direct effect of UVA on proximal HF keratinocytes.

Most of UV-related effects in the HFs could be seen only after high dose transepidermal UVR (50 J/cm² UVA and 50 mJ/cm² UVB), i.e. reduction of HF ORS keratinocyte proliferation, stimulation of cells apoptosis throughout the whole HF ORS and HM. However, some UV-related effects could be already seen after low-dose (10 J/cm² UVA and 20 mJ/cm² UVB) UV radiation, i.e. modulation of growth factors (IGF-1, TGF- β 2) related to hair growth, induction of oxidative damage (8-OH-dG), HF cytotoxicity and dystrophy (melanin clumping). The high UV radiation dose leads to severe tissue and HF damage, which renders tissue sectioning very difficult, and possibly leads to artefacts. For example, it was not possible to evaluate the HF cytotoxicity/dystrophy in high-dose UV-irradiated HFs by counting the number of melanin clumps in the hair bulb because most of the HFs turned prematurely into catagen, which hair cycle phase is characterized by termination of melanin production (64). Also the unchanged 8-OH-dG expression after high UV-irradiation may be an artefact due to the high amounts of DNA destruction (30). Therefore, intermediate UVA and UVB doses (40 J/cm² UVA and 40 mJ/cm² UVB) were used for the subsequent caffeine protection experiment.

In our *ex vivo* assay, transepidermal UV radiation slightly promotes catagen within intact human skin, although this effect is only seen after treatment with high UV dose. In light of this, the slight differences in apoptosis and regulation of hair cycle growth factors, as observed after low UV radiation in proximal ORS keratinocytes, appear irrelevant and not enough to induce premature catagen development. In contrast, high UV radiation induces significant HM keratinocyte apoptosis, down-regulation of IGF-1 and up-regulation of TGF- β 2 in the proximal ORS, a chain of events that leads to catagen induction. Interestingly, low UV dose treatment may even maintain longer anagen phase *ex vivo*. Thus, the current *ex vivo* model, mimics the previously reported differential effects of UVR on hair growth *in vivo*, i.e. that different duration of UV exposure can be either hair growth-promoting or inhibitory in mice.

It is reported that mast cells can be directly or indirectly affected by UV radiation (75–77). Our study contributes to the field by showing that the number of histochemically detectable perifollicular mast cells is decreased while their degranulation is increased 1 day after irradiation of the skin surface with UVA and UVB. Therefore, mast cells are either directly or indirectly activated by UV radiation, as the observed reduced number can be explained by the fact that the mast cells are completely degranulated and thus hardly detectable by histochemistry. Interestingly, the UV-mediated activation of mast cells occurs not only in the papillary and reticular of the dermis but also deep in the subcutis. Since the activation of mast cells play a role also in catagen development, at least in mice (72), but likely also in human HFs (73), it is conceivable that UV-induced mast cell degranulation may contribute to premature HF regression.

With our *ex vivo* full thickness skin organ culture model, we could confirm previously published results obtained in UVB-treated microdissected HFs *ex vivo* (30), e.g. increased LDH-release with increasing UVB-doses representing necrosis, increased HM keratinocyte apoptosis, induction of catagen, increase in TGF- β 2 expression, and increase in mast cell degranulation. However, considering that UVB tends to be completely absorbed by the epidermis (2, 4, 55), it is plausible that it was mainly UVA irradiation that exerted these effects in our improved irradiated full thickness skin organ culture *ex vivo*.

Importantly, our experiments show that the topical application of 0.1% caffeine in male occipital scalp skin protects HFs from some unwanted effects induced by UV radiation (UVA+UVB). One can speculate that additional important beneficial effects of caffeine to UVR-mediated damage may have been hidden by the experimental set-up chosen in order to imitate consumer's behaviour, since day 4 of culture may represent a suboptimal time point for the irradiation because the skin may already started to degenerate spontaneously. In spite of this, we could show that caffeine treatment alleviates UV-mediated HF cytotoxicity and dystrophy, keratinocyte apoptosis in the distal and central ORS, and increased expression of TGF- β 2 in the proximal ORS.

Caffeine is a potent antioxidant (89) which also increases cAMP synthesis by inhibiting phosphodiesterase activity (59). It is conceivable that these caffeine activities contribute to UVR-mediated HF protection, as other compounds that raise cAMP levels, such as alpha-melanocyte stimulating hormone (90, 91), reduce UVR-mediated apoptosis and DNA damage.

It is not clear though whether caffeine protected or rescued HFs from UV-mediated damage as we have adapted the continuous daily administration of caffeine during the culture period, i.e. 3 days prior to and for 3 consecutive days after UV exposure with 40 J/cm² UVA + 40 mJ/cm² UVB. Of note, the fact that caffeine reduces UVR-induced keratinocyte proliferation in the central ORS, may indicate a rescue system for bulge stem cells located in the ORS basal layer of central HF epithelium, whose increased proliferation has been associated with their depletion after chemotherapy induced-cytotoxicity (38) or inflammation (92).

Although this was not the main aim of the current project, our results also provide further insights into the effects of topical caffeine on human skin and HF homeostasis. Although it is known that caffeine does not induce skin or HF cytotoxicity, and up-regulates the expression of the anagen-promoting growth factor IGF-1, we show here for the first time that this also applies to topical application of caffeine to human skin *ex vivo*. However, contrary to

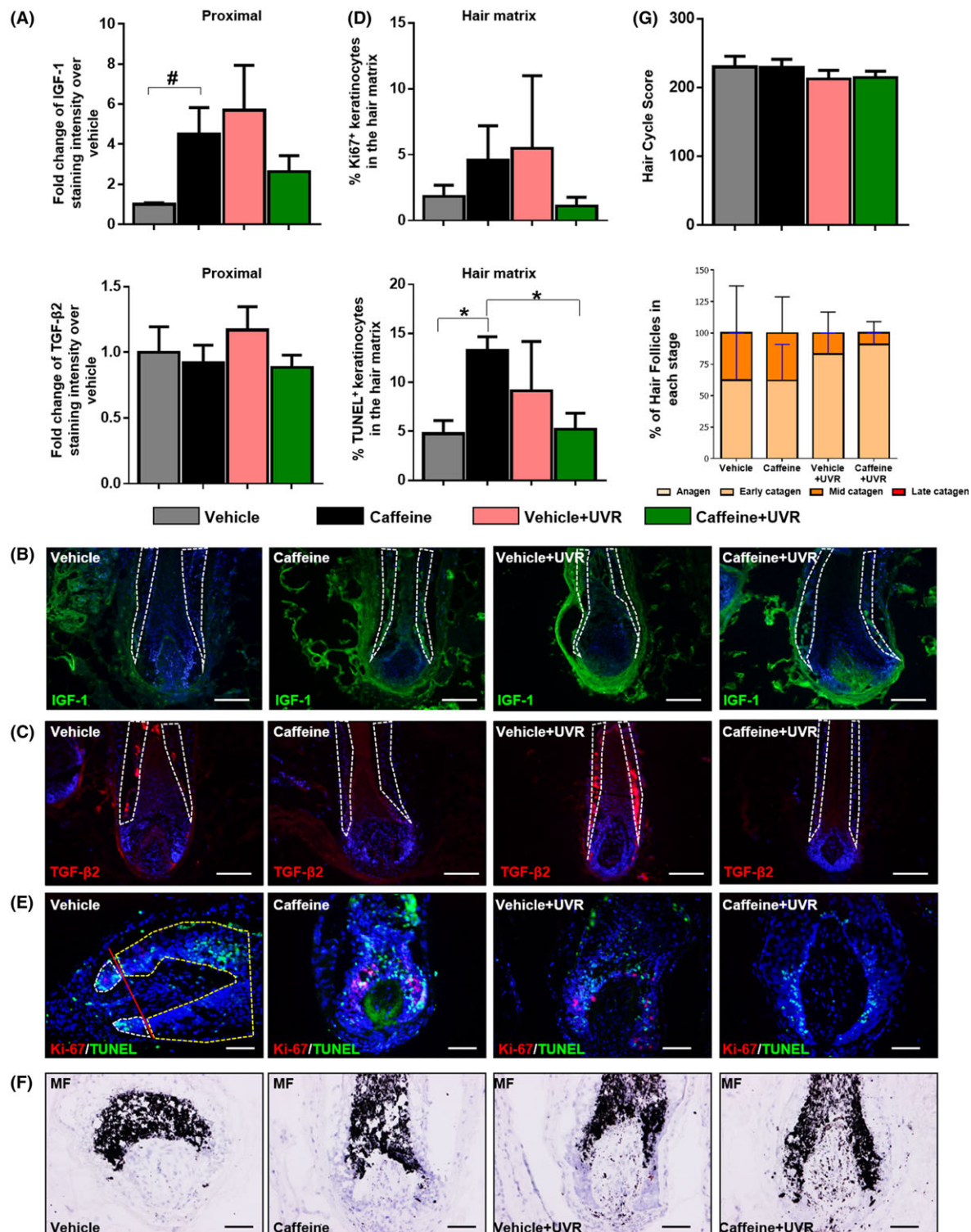


Figure 10 Single treatment of caffeine or UVR differentially impacts on hair cycle-associated parameters but their combination restores baseline levels, thereby not affecting hair cycle *ex vivo*. (A) Quantitative analysis of IGF-1 and TGF- β 2 expression in proximal ORS of vehicle, caffeine, vehicle+UVR or caffeine+UVR treated HFs. Relative staining intensity was measured using ImageJ. Data are expressed as fold-change of IGF-1 or TGF- β 2 staining intensity in treated samples over sham. Mean \pm SEM $n = 4\text{--}13$ for proximal ORS evaluation areas analysed from two skin punches per experimental group from two donors, IGF-1: Kruskal-Wallis test, ns, Mann-Whitney test, $^{\#}P < 0.05$, TGF- β 2: Kruskal-Wallis test, ns. (B) Representative images showing IGF-1 (green) expression in the proximal hair follicle ORS. (C) Representative images showing TGF- β 2 (red) expression in the proximal hair follicle ORS. (D) Quantitative analysis of the % of Ki-67 $^{+}$ or TUNEL $^{+}$ keratinocytes in the HM of vehicle, caffeine, vehicle+UVR or caffeine+UVR treated HFs. The number and % of Ki-67 $^{+}$ or TUNEL $^{+}$ keratinocytes was counted respectively below the Auber's line or within the whole HM (yellow line) among all DAPI $^{+}$ cells. Data are expressed as % of Ki-67 $^{+}$ or TUNEL $^{+}$ cells, Mean \pm SEM $n = 3\text{--}9$ for Ki-67 and TUNEL HFs analysed from two skin punches per experimental group from two donors, Ki-67: Kruskal-Wallis test, ns, TUNEL: Kruskal-Wallis test $P < 0.05$ and Dunn's test: $^{\ast}P < 0.05$. Hair cycle analyses was performed using (E) Ki-67/TUNEL immunohistochemistry and (F) Masson Fontana histochemistry. (E) Representative images showing Ki-67 (red) and TUNEL (green) positive cells in the HM. (F) Representative images showing HFs stained with Masson Fontana. (G) For the hair cycle score, arbitrary units were used to define anagen (100), early catagen (200), mid catagen (300) and late catagen (400). For hair follicle staging, % number of HFs in each stage is presented. Data are expressed as Mean \pm SEM $n = 8\text{--}17$ HFs for hair cycle score and $n = 2$ from 8 to 17 HFs for HF stage analysed from two skin punches per experimental group from two donors, Kruskal-Wallis test, ns. Dotted lines indicate the reference areas used for evaluation (B, C, E). Hair matrix keratinocyte proliferation was evaluated only within the area limited by the white dotted line, while hair matrix keratinocyte apoptosis was evaluated within the area limited by the white and yellow dotted lines (E). Scale bars: 50 μ m.

our previous published results using microdissected HFs and different concentrations of this nutraceutical, the topical application of 0.1% caffeine did not rescue HM cell apoptosis but instead promoted it, and did not maintain longer anagen *ex vivo*. Yet, it is conceivable that the amount of caffeine that reached the hair bulb after topical application may have been too high or too low, given that only defined concentrations of caffeine positively modulates human hair growth *ex vivo*, with great gender-dependent differences (58). Therefore, our study reinforces that particular attention must be placed on selecting the concentration of caffeine very carefully for topical hair care formulations.

Conclusions

In conclusions, we show here for the first time that transepidermal UV radiation negatively affected HF functions: it triggers HF cytotoxicity, dystrophy, oxidative DNA damage, reduces keratinocyte proliferation and increases their apoptosis, stimulates TGF- β 2 and decreases in IGF-1 protein expression in ORS keratinocytes, premature catagen development, and perifollicular mast cell degranulation. While UV-mediated damage was present throughout the HF length, it was more prominent in the distal HF epithelium. Moreover, we show here that the transepidermal UVR irradiation of full thickness, organ-cultured human scalp skin closely mimics the *in vivo* situation. Finally, our study demonstrates that the topical application of 0.1% caffeine protects human scalp HFs from UVR-mediated damage: namely it alleviates UV-mediated HF cytotoxicity and dystrophy, HF keratinocyte apoptosis in the distal and central ORS, and the increase of TGF- β 2 expression in the proximal ORS. Therefore, it is meaningful to integrate cosmeceuticals or

nutraceuticals, such as caffeine, that are able to protect scalp HFs from UVR into sunscreen formulations.

Acknowledgements

This study was supported by a research grant from DR. KURT WOLFF GMBH & CO. KG., Bielefeld, Germany, to Monasterium Laboratory GmbH, Münster, Germany. The excellent technical assistance of Janine Jakobs, Maria Udriste, Laura Christina Nicolae, Sara Quinones are gratefully acknowledged, and we thank arrows biomedical Deutschland GmbH, Münster, for allowing us the use of their plate reader.

Author contributions

R.P. conceived the study. M.B. and R.P. designed the study and obtained funding. M.B. supervised the study, interpreted the results assisted by J.G., J.W., C.W., and R.P., and wrote the manuscript with input from J.G., J.W., N.B., R.P., J.G., and J.W. performed most of the experiments, and analysed the data, assisted by J.C., S.G., M.A. and J.L., F.J., and W.F. provided human samples, and M.Bö. provided the UV lamps and photo dermatology advice. The manuscript was edited and approved by all authors.

Conflict of interest

M.B., J.G., J.W., J.C., S.G., J.L. are or were employees of Monasterium Laboratory (ML) GmbH, Münster, a biotech company performing contracted skin and hair research projects. ML was founded by R.P., and C.W. and N.B. serve as consultants for ML.

References

- Dunaway, S., Odin, R., Zhou, L., Ji, L., Zhang, Y. and Kadekaro, A.L. Natural antioxidants: multiple mechanisms to protect skin from solar radiation. *Front. Pharmacol.* **9**, 392 (2018).
- Pérez-Sánchez, A., Barrajón-Catalán, E., Herranz-López, M. and Micol, V. Nutraceuticals for skin care: a comprehensive review of human clinical studies. *Nutrients* **10**, E403 (2018).
- Slominski, A.T., Zmijewski, M.A., Plonka, P.M., Szafarski, J.P. and Paus, R. How UV light touches the brain and endocrine system through skin, and why. *Endocrinology* **159**, 1992–2007 (2018).
- Garmyn, M., Young, A.R. and Miller, S.A. Mechanisms of and variables affecting UVR photopadaptation in human skin. *Photochem. Photobiol. Sci.* **17**, 1932–1940 (2018).
- McDaniel, D., Farris, P. and Valacchi, G. Atmospheric skin aging-Contributors and

- inhibitors. *J. Cosmet. Dermatol.* **17**, 124–137 (2018).
6. Jablonski, N.G. and Chaplin, G. The roles of vitamin D and cutaneous vitamin D production in human evolution and health. *Int. J. Paleopathol.* **23**, 54–59 (2018).
 7. Kamenisch, Y., Ivanova, I., Drexler, K. and Berneburg, M. UVA, metabolism and melanoma: UVA makes melanoma hungry for metastasis. *Exp. Dermatol.* **27**, 941–949 (2018).
 8. Mullenders, L.H.F. Solar UV damage to cellular DNA: from mechanisms to biological effects. *Photochem. Photobiol. Sci.* **17**, 1842–1852 (2018).
 9. Janjetovic, Z., Nahmias, Z.P., Hanna, S., Jarrett, S.G., Kim, T.-K., Reiter, R.J., Slominski, A.T. Melatonin and its metabolites ameliorate ultraviolet B-induced damage in human epidermal keratinocytes. *J. Pineal Res.* **57**, 90–102 (2014).
 10. Janjetovic, Z., Jarrett, S.G., Lee, E.F., Duprey, C., Reiter, R.J. and Slominski, A.T. Melatonin and its metabolites protect human melanocytes against UVB-induced damage: Involvement of NRF2-mediated pathways. *Sci. Rep.* **7**, 1274 (2017).
 11. Kleszczyński, K., Zwicker, S., Tukaj, S. et al. Melatonin compensates silencing of heat shock protein 70 and suppresses ultraviolet radiation-induced inflammation in human skin ex vivo and cultured keratinocytes. *J. Pineal Res.* **58**, 117–126 (2015).
 12. Emri, G., Paragh, G., Tósaki, Á. et al. Ultraviolet radiation-mediated development of cutaneous melanoma: an update. *J. Photochem. Photobiol. B* **185**, 169–175 (2018).
 13. Kwon, T.-R., Kim, J.H., Hong, J.-Y. et al. Irradiation with 310 nm and 340 nm ultraviolet light-emitting-diodes can improve atopic dermatitis-like skin lesions in NC/Nga mice. *Photochem. Photobiol. Sci.* **17**, 1127–1135 (2018).
 14. Nguyen, N.T. and Fisher, D.E. MITF and UV responses in skin: from pigmentation to addiction. *Pigment Cell Melanoma Res.* **32**, 224–236 (2018).
 15. Pain, S., Berthélémy, N., Naudin, C., Degraeve, V. and André-Frei, V. Understanding solar skin elastosis—cause and treatment. *J. Cosmet. Sci.* **69**, 175–185 (2018).
 16. Sonnenheimer, K. and Krutmann, J. Novel means for photoprotection. *Front. Med. (Lausanne)* **5**, 162 (2018).
 17. Uco, D.P., Leite-Silva, V.R., Silva, H.D.T. et al. UVA and UVB formulation phototoxicity in a three-dimensional human skin model: photodegradation effect. *Toxicol. In Vitro* **26**, 37–44 (2018).
 18. Trüb, R.M. The impact of oxidative stress on hair. *Int. J. Cosmet. Sci.* **37**(Suppl 2), 25–30 (2015).
 19. Trüb, R.M. Effect of ultraviolet radiation, smoking and nutrition on hair. *Curr. Probl. Dermatol.* **47**, 107–120 (2015).
 20. França, K., Castillo, D., Tchernev, G. and Lotti, T. UVA-1 in the treatment of alopecia areata. *Dermatol. Ther.* **30**, e12547 (2017).
 21. Borgia, F., Giuffrida, R., Lentini, M., Palazzo, R. and Cannavò, S.P. Follicular mucinosis with diffuse scalp alopecia treated with narrow-band UVB phototherapy: the role of trichoscopy in monitoring therapeutic outcomes. *G. Ital. Dermatol. Venereol.* **151**, 212–215 (2016).
 22. Darwin, E., Arora, H., Hirt, P.A., Wikramanayake, T.C. and Jimenez, J.J. A review of monochromatic light devices for the treatment of alopecia areata. *Lasers Med. Sci.* **33**, 435–444 (2018).
 23. Darwin, E., Heyes, A., Hirt, P.A., Wikramanayake, T.C. and Jimenez, J.J. Low-level laser therapy for the treatment of androgenic alopecia: a review. *Lasers Med. Sci.* **33**, 425–434 (2018).
 24. Braun, S., Krampert, M., Bodó, E. et al. Keratinocyte growth factor protects epidermis and hair follicles from cell death induced by UV irradiation, chemotherapeutic or cytotoxic agents. *J. Cell Sci.* **119**, 4841–4849 (2006).
 25. Jeong, Y.-M., Sung, Y.K., Kim, W.-K. et al. Ultraviolet B preconditioning enhances the hair growth-promoting effects of adipose-derived stem cells via generation of reactive oxygen species. *Stem Cells Dev.* **22**, 158–168 (2013).
 26. Johnson, B.E. Potentiation of hair-growth by ultra-violet light. *Nature* **9**, 159–160 (1960).
 27. Johnson, B.E. and Daniels, F. Lysosomes and the reactions of skin to ultraviolet radiation. *J. Invest. Dermatol.* **53**, 85–94 (1969).
 28. Müller-Röver, S., Rossiter, H., Paus, R., Handjiski, B., Peters, E.M., Murphy, J.E. et al. Overexpression of Bcl-2 protects from ultraviolet B-induced apoptosis but promotes hair follicle regression and chemotherapy-induced alopecia. *Am. J. Pathol.* **156**, 1395–1405 (2000).
 29. Ferguson, B., Kunisada, T., Aoki, H., Handoko, H.Y. and Walker, G.J. Hair follicle melanocyte precursors are awoken by ultraviolet radiation via a cell extrinsic mechanism. *Photochem. Photobiol. Sci.* **14**, 1179–1189 (2015).
 30. Lu, Z., Fischer, T.W., Hasse, S. et al. Profiling the response of human hair follicles to ultraviolet radiation. *J. Invest. Dermatol.* **129**, 1790–1804 (2009).
 31. Cha, H.J., Kim, O.-Y., Lee, G.T. et al. Identification of ultraviolet B radiation-induced microRNAs in normal human dermal papilla cells. *Mol. Med. Rep.* **10**, 1663–1670 (2014).
 32. Lu, Z., Hasse, S., Bodo, E., Rose, C., Funk, W. and Paus, R. Towards the development of a simplified long-term organ culture method for human scalp skin and its appendages under serum-free conditions. *Exp. Dermatol.* **16**, 37–44 (2007).
 33. Bodó, E., Kany, B., Gáspár, E. et al. Thyroid-stimulating hormone, a novel, locally produced modulator of human epidermal functions, is regulated by thyrotropin-releasing hormone and thyroid hormones. *Endocrinology* **151**, 1633–1642 (2010).
 34. Vidali, S., Chéret, J., Giesen, M. et al. Thyroid hormones enhance mitochondrial function in human epidermis. *J. Invest. Dermatol.* **136**, 2003–2012 (2016).
 35. Haslam, I.S., Hardman, J.A. and Paus, R. Topically applied nicotinamide inhibits human hair follicle growth ex vivo. *J. Invest. Dermatol.* **138**, 1420–1422 (2018).
 36. Gladý, A., Tanaka, M., Moniaga, C.S., Yasui, M. and Hara-Chikuma, M. Involvement of NADPH oxidase 1 in UVB-induced cell signaling and cytotoxicity in human keratinocytes. *Biochem. Biophys. Rep.* **14**, 7–15 (2018).
 37. Bayerl, C., Taake, S., Moll, I. and Jung, E.G. Characterization of sunburn cells after exposure to ultraviolet light. *Photodermatol. Photomed. Photomed.* **11**, 149–154 (1995).
 38. Bodó, E., Tobin, D.J., Kamenisch, Y. et al. Dissecting the impact of chemotherapy on the human hair follicle: a pragmatic in vitro assay for studying the pathogenesis and potential management of hair follicle dystrophy. *Am. J. Pathol.* **171**, 1153–1167 (2007 Oct).
 39. Langan, E.A., Philpott, M.P., Kloepper, J.E. and Paus, R. Human hair follicle organ culture: theory, application and perspectives. *Exp. Dermatol.* **24**, 903–911 (2015).
 40. Oláh, A., Gherardini, J., Bertolini, M. et al. The thyroid hormone analogue KB2115 (Eprotirome) prolongs human hair growth (Anagen) ex vivo. *J. Invest. Dermatol.* **136**, 1711–1714 (2016).
 41. Purba, T.S., Brunkin, L., Peake, M. et al. Characterisation of cell cycle arrest and terminal differentiation in a maximally proliferative human epithelial tissue: lessons from the human hair follicle matrix. *Eur. J. Cell Biol.* **96**, 632–641 (2017).
 42. Bertolini, M., Zilio, F., Rossi, A. et al. Abnormal interactions between perifollicular mast cells and CD8 + T-cells may contribute to the pathogenesis of alopecia areata. *PLoS ONE* **9**, e94260 (2014).

43. Flori, E., Mastrofrancesco, A., Kovacs, D. et al. 2,4,6-Octatrienoic acid is a novel promoter of melanogenesis and antioxidant defence in normal human melanocytes via PPAR- γ activation. *Pigment Cell Melanoma Res.* **24**, 618–630 (2011).
44. Bussoletti, C., Tolaini, M.V. and Celeno, L. Efficacy of a cosmetic phyto-caffeine shampoo in female androgenetic alopecia. *G Ital Dermatol Venereol.* [Epub ahead of print] (2018).
45. Davis, M.G., Thomas, J.H., van de Velde, S. et al. A novel cosmetic approach to treat thinning hair. *Br. J. Dermatol.* **165**, 24–30 (2011).
46. Jung, I.K., Park, S.C., Lee, Y.R. et al. Development of a stiffness-angle law for simplifying the measurement of human hair stiffness. *Int. J. Cosmet. Sci.* **40**, 157–164 (2018).
47. Abe, A., Saito, M., Kadhum, W.R., Todo, H. and Sugabayashi, K. Establishment of an evaluation method to detect drug distribution in hair follicles. *Int. J. Pharm.* **542**, 27–35 (2018).
48. Otberg, N., Patzelt, A., Rasulev, U. et al. The role of hair follicles in the percutaneous absorption of caffeine. *Br. J. Clin. Pharmacol.* **65**, 488–492 (2008 Apr).
49. Otberg, N., Teichmann, A., Rasuljev, U., Sinkgraven, R., Sterry, W. and Lademann, J. Follicular penetration of topically applied caffeine via a shampoo formulation. *Skin Pharmacol. Physiol.* **20**, 195–198 (2007).
50. Trauer, S., Patzelt, A., Otberg, N. et al. Permeation of topically applied caffeine through human skin – a comparison of in vivo and in vitro data. *Br. J. Clin. Pharmacol.* **68**, 181–186 (2009).
51. Trauer, S., Lademann, J., Knorr, F. et al. Development of an in vitro modified skin absorption test for the investigation of the follicular penetration pathway of caffeine. *Skin Pharmacol. Physiol.* **23**, 320–327 (2010).
52. Conney, A.H., Lu, Y.-P., Lou, Y.-R. and Huang, M.-T. Inhibitory effects of tea and caffeine on UV-induced carcinogenesis: relationship to enhanced apoptosis and decreased tissue fat. *Eur. J. Cancer Prev.* **11** (Suppl 2), S28–S36 (2002).
53. Hebbar, S.A., Mitra, A.K., George, K.C. and Verma, N.C. Caffeine ameliorates radiation-induced skin reactions in mice but does not influence tumour radiation response. *J. Radiol. Prot.* **22**, 63–69 (2002).
54. Heffernan, T.P., Kawasumi, M., Blasina, A., Anderes, K., Conney, A.H. and Nghiem, P. ATR-Chk1 pathway inhibition promotes apoptosis after UV treatment in primary human keratinocytes: potential basis for the UV protective effects of caffeine. *J. Invest. Dermatol.* **129**, 1805–1815 (2009).
55. McDaniel, D.H., Mazur, C., Wortzman, M.S. and Nelson, D.B. Efficacy and tolerability of a double-conjugated retinoid cream vs 1.0% retinol cream or 0.025% tretinoin cream in subjects with mild to severe photoaging. *J. Cosmet. Dermatol.* **16**, 542–548 (2017).
56. Zajdela, F. and Latarjet, R. Inhibition of skin carcinogenesis in vivo by caffeine and other agents. *Natl Cancer Inst. Monogr.* **50**, 133–140 (1978).
57. Fischer, T.W., Hippler, U.C. and Elsner, P. Effect of caffeine and testosterone on the proliferation of human hair follicles in vitro. *Int. J. Dermatol.* **46**, 27–35 (2007).
58. Fischer, T.W., Herczeg-Lisztes, E., Funk, W., Zillikens, D., Bíró, T. and Paus, R. Differential effects of caffeine on hair shaft elongation, matrix and outer root sheath keratinocyte proliferation, and transforming growth factor- β 2/insulin-like growth factor-1-mediated regulation of the hair cycle in male and female human hair follicles in vitro. *Br. J. Dermatol.* **171**, 1031–1043 (2014).
59. Herman, A. and Herman, A.P. Caffeine's mechanisms of action and its cosmetic use. *Skin Pharmacol. Physiol.* **26**, 8–14 (2013).
60. Dhurat, R., Chitallia, J., May, T.W. et al. An open-label randomized multicenter study assessing the noninferiority of a caffeine-based topical liquid 0.2% versus minoxidil 5% solution in male androgenetic alopecia. *Skin Pharmacol. Physiol.* **30**, 298–305 (2017).
61. Alonso, C., Carrer, V., Barba, C. and Coderch, L. Caffeine delivery in porcine skin: a confocal Raman study. *Arch. Dermatol. Res.* **310**, 657–664 (2018).
62. Paus, R., Rosenbach, T., Haas, N. and Czarnetzki, B.M. Patterns of cell death: the significance of apoptosis for dermatology. *Exp. Dermatol.* **2**, 3–11 (1993).
63. Lin, J.Y. and Fisher, D.E. Melanocyte biology and skin pigmentation. *Nature* **445**, 843–850 (2007).
64. Oh, J.W., Kloepper, J., Langan, E.A. et al. A guide to studying human hair follicle cycling in vivo. *J. Invest. Dermatol.* **136**, 34–44 (2016).
65. Samuelov, L., Kinori, M., Bertolini, M. and Paus, R. Neural controls of human hair growth: calcitonin gene-related peptide (CGRP) induces catagen. *J. Dermatol. Sci.* **67**, 153–155 (2012).
66. Mamalis, A., Fiadorchanka, N., Adams, L. et al. An immunohistochemical panel to assess ultraviolet radiation-associated oxidative skin injury. *J. Drugs Dermatol.* **13**, 574–578 (2014).
67. Fernández, E., Barba, C., Alonso, C., Martí, M., Parra, J.L. and Coderch, L. Photodamage determination of human hair. *J. Photochem. Photobiol. B* **5**, 101–106 (2012).
68. Chen, C., Xu, Y. and Song, Y. IGF-1 gene-modified muscle-derived stem cells are resistant to oxidative stress via enhanced activation of IGF-1R/PI3K/AKT signaling and secretion of VEGF. *Mol. Cell. Biochem.* **386**, 167–175 (2014).
69. Tarantini, S., Valcarcel-Ares, N.M., Yabluchanskiy, A. et al. Insulin-like growth factor 1 deficiency exacerbates hypertension-induced cerebral microhemorrhages in mice, mimicking the aging phenotype. *Aging Cell* **16**, 469–479 (2017).
70. Xu, L., Zhang, W., Sun, R. et al. IGF-1 may predict the severity and outcome of patients with sepsis and be associated with micro-RNA-1 level changes. *Exp. Ther. Med.* **14**, 797–804 (2017).
71. Paus, R., Maurer, M., Slominski, A. and Czarnetzki, B.M. Mast cell involvement in murine hair growth. *Dev. Biol.* **163**, 230–240 (1994).
72. Maurer, M., Fischer, E., Handjiski, B. et al. Activated skin mast cells are involved in murine hair follicle regression (catagen). *Lab. Invest.* **77**, 319–332 (1997).
73. Peters, E.M.J., Liotiri, S., Bodó, E. et al. Probing the effects of stress mediators on the human hair follicle: substance P holds central position. *Am. J. Pathol.* **171**, 1872–1886 (2007).
74. Jadkauskaitė, L., Bahri, R., Farjo, N. et al. Nuclear factor (erythroid-derived 2)-like-2 pathway modulates substance P-induced human mast cell activation and degranulation in the hair follicle. *J. Allergy Clin. Immunol.* **142**, 1331–1333 (2018).
75. Kim, M.-S., Kim, Y.K., Lee, D.H. et al. Acute exposure of human skin to ultraviolet or infrared radiation or heat stimuli increases mast cell numbers and tryptase expression in human skin in vivo. *Br. J. Dermatol.* **160**, 393–402 (2009).
76. Siiskonen, H., Smorodchenko, A., Krause, K. and Maurer, M. Ultraviolet radiation and skin mast cells: effects, mechanisms and relevance for skin diseases. *Exp. Dermatol.* **27**, 3–8 (2018).
77. Del Pozo, J., Pimentel, M.T.Y., Paradela, S., Almagro, M., Martínez, W. and Fonseca, E. Anetodermic mastocytosis: response to PUVA therapy. *J. Dermatolog. Treat.* **18**, 184–187 (2007).
78. Conney, A.H., Lu, Y.-P., Lou, Y.-R., Kawasumi, M. and Nghiem, P. Mechanisms of caffeine-induced inhibition of UVB carcinogenesis. *Front. Oncol.* **3**, 144 (2013).

79. Balasaraswathy, P., Kumar, U., Srinivas, C.R. and Nair, S. UVA and UVB in sunlight, optimal utilization of UV rays in sunlight for phototherapy. *Indian J. Dermatol. Venereol. Leprol.* **68**, 198–201 (2002).
80. Ichihashi, M. and Ando, H. The maximal cumulative solar UVB dose allowed to maintain healthy and young skin and prevent premature photoaging. *Exp. Dermatol.* **23** (Suppl 1), 43–46 (2014).
81. Moyal, D., Chardon, A. and Kollias, N. UVA protection efficacy of sunscreens can be determined by the persistent pigment darkening (PPD) method. (Part 2). *Photodermatol. Photoimmunol. Photomed.* **16**, 250–255 (2000).
82. O'Neill, C.M., Kazantzidis, A., Ryan, M.J. et al. Seasonal changes in vitamin D-effective UVB availability in Europe and associations with population serum 25-hydroxyvitamin D. *Nutrients.* **8**, E533 (2016).
83. Dario, M.F., Baby, A.R. and Velasco, M.V.R. Effects of solar radiation on hair and photoprotection. *J. Photochem. Photobiol. B* **153**, 240–246 (2015).
84. Huang, X., Protheroe, M.D., Al-Jumaily, A.M., Paul, S.P. and Chalmers, A.N. Review of human hair optical properties in possible relation to melanoma development. *J. Biomed. Opt.* **23**, 1–9 (2018).
85. Marsh, J.M., Davis, M.G., Lucas, R.L. et al. Preserving fibre health: reducing oxidative stress throughout the life of the hair fibre. *Int. J. Cosmet. Sci.* **37**(Suppl 2), 16–24 (2015).
86. Bäslér, K., Bergmann, S., Heisig, M., Naegel, A., Zorn-Kruppa, M. and Brandner, J.M. The role of tight junctions in skin barrier function and dermal absorption. *J. Control Release.* **28**, 105–118 (2016).
87. Dahlhoff, M., Camera, E., Schäfer, M. et al. Sebaceous lipids are essential for water repulsion, protection against UVB-induced apoptosis and ocular integrity in mice. *Development.* **143**, 1823–1831 (2016).
88. Stough, D., Stenn, K., Haber, R. et al. Psychological effect, pathophysiology, and management of androgenetic alopecia in men. *Mayo Clin. Proc.* **80**, 1316–1322 (2005).
89. Salomone, F., Galvano, F. and Li Volti, G. Molecular bases underlying the hepatoprotective effects of coffee. *Nutrients.* **9**, E85 (2017).
90. Kokot, A., Metze, D., Mouchet, N. et al. Alpha-melanocyte-stimulating hormone counteracts the suppressive effect of UVB on Nrf2 and Nrf-dependent gene expression in human skin. *Endocrinology* **150**, 3197–3206 (2009).
91. Böhm, M., Wolff, I., Scholzen, T.E. et al. alpha-Melanocyte-stimulating hormone protects from ultraviolet radiation-induced apoptosis and DNA damage. *J. Biol. Chem.* **280**, 5795–5802 (2005).
92. Harries, M.J., Meyer, K., Chaudhry, I., EKlopper, J., Poblet, E., Griffiths, C.E., Paus, R. Lichen planopilaris is characterized by immune privilege collapse of the hair follicle's epithelial stem cell niche. *J. Pathol.* **231**, 236–247 (2013).